

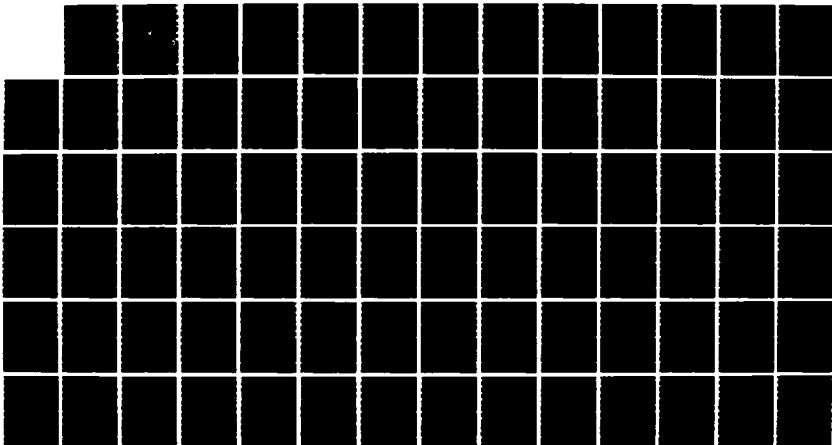
AD-A178 857

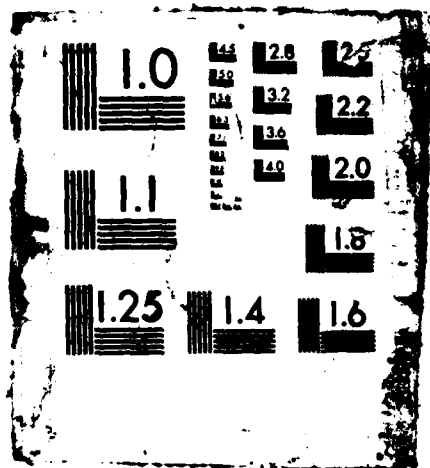
SHIPBOARD COMBAT SURVIVABLE HF ANTENNA DESIGNS(U) NAVAL
POSTGRADUATE SCHOOL MONTEREY CA I G VORRIAS DEC 86
NPS-62-86-006

1/1

UNCLASSIFIED

F/G 17/2 1 NL





DTIC FILE COPY

2

NPS-62-86-006

AD-A178 857

NAVAL POSTGRADUATE SCHOOL Monterey, California



THESIS

SHIPBOARD COMBAT SURVIVABLE HF ANTENNA
DESIGNS

by

Ioannis G. Vorrias

December 1986

Thesis Advisor

Richard W. Adler

DTIC
ELECTE
APR 8 1987
S A D

Approved for public release; distribution is unlimited.

Prepared for:
Naval Ocean Systems Center
San Diego, CA 92152

87

4 7 - 1 4 3

REPRODUCED AT GOVERNMENT EXPENSE

NAVAL POSTGRADUATE SCHOOL
Monterey, CA 93943-5000

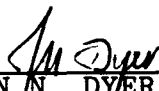
Rear Admiral R. C. Austin
Superintendent

D. A. Schradly
Provost

This thesis is prepared in conjunction with research sponsored in part by Naval Ocean Systems Center under NPS-62-86-006.

Reproduction of all or part of this report is authorized.

Released By:



JOHN N. DYER
Dear of Science and Engineering

REPORT DOCUMENTATION PAGE

REPRODUCED AT GOVERNMENT EXPENSE

1a REPORT SECURITY CLASSIFICATION UNCLASSIFIED		1b RESTRICTIVE MARKINGS	
2a SECURITY CLASSIFICATION AUTHORITY		3 DISTRIBUTION/AVAILABILITY OF REPORT Approved for for public release; distribution is unlimited	
2b DECLASSIFICATION/DOWNGRADING SCHEDULE			
4 PERFORMING ORGANIZATION REPORT NUMBER(S) NPS-62-86-006		5 MONITORING ORGANIZATION REPORT NUMBER(S)	
6a NAME OF PERFORMING ORGANIZATION Naval Postgraduate School	6b OFFICE SYMBOL (if applicable) 62	7a NAME OF MONITORING ORGANIZATION Naval Ocean Systems Center	
6c ADDRESS (City, State, and ZIP Code) Monterey, California 93943-5000		7b ADDRESS (City, State, and ZIP Code) San Diego, California 92152	
8a NAME OF FUNDING/SPONSORING ORGANIZATION Naval Ocean Systems Cntr	8b OFFICE SYMBOL (if applicable) Code 825	9 PROCUREMENT INSTRUMENT IDENTIFICATION NUMBER	
8c ADDRESS (City, State, and ZIP Code) San Diego, California 92152		10 SOURCE OF FUNDING NUMBERS	
		PROGRAM ELEMENT NO	PROJECT NO
11 TITLE (include Security Classification) SHIPBOARD COMBAT SURVIVABLE HF ANTENNA DESIGNS			
12 PERSONAL AUTHOR(S) Vorrias, Ioannis G.			
13a TYPE OF REPORT Master's Thesis	13b TIME COVERED FROM _____ TO _____	14 DATE OF REPORT (Year Month Day) 1986 December	15 PAGE COUNT 81
16 SUPPLEMENTARY NOTATION			
17 COSATI CODES		18 SUBJECT TERMS (Continue on reverse if necessary and identify by block number) Combat Survivable Antenna; Computer Modeling of Antennas	
FIELD	GROUP		
19 ABSTRACT (Continue on reverse if necessary and identify by block number) This thesis investigates the feasibility of two shipboard combat survivable HF communication antenna designs. Both antennas are modeled as a rectangular volume, which in one case is excited by a square patch atop a monopole, placed at various spacings from the center of one of the volume's faces, and in the other case is excited by a wire which is connected between the center of a face that is created by a rectangular shaped notch and a perfect ground plane. Several computer models of the two configurations for either different spacings between the patch monopole and the rectangular volume, or different notch sizes, are modeled with the Numerical Electromagnetics Code (NEC) and compared. Input impedances and radiation patterns of the two survivable antennas are presented. Both antennas are evaluated against a 3:1 Standing Wave Ratio (SWR) criterion.			
20 DISTRIBUTION/AVAILABILITY OF ABSTRACT <input type="checkbox"/> UNCLASSIFIED/UNLIMITED <input checked="" type="checkbox"/> SAME AS RPT <input type="checkbox"/> OTC USERS		21 ABSTRACT SECURITY CLASSIFICATION UNCLASSIFIED	
22a NAME OF RESPONSIBLE INDIVIDUAL Prof Richard W. Adler		22b TELEPHONE (include Area Code) (408) 646-2352	22c OFFICE SYMBOL 62Ab

Approved for public release; distribution is unlimited.

Shipboard Combat Survivable HF Antenna Designs

by

Ioannis G. Vorrias
Lieutenant, Hellenic Navy
B.S., Hellenic Naval Academy, 1977

Submitted in partial fulfillment of the
requirements for the degree of

MASTER OF SCIENCE IN ELECTRICAL ENGINEERING

from the

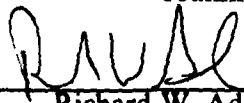
NAVAL POSTGRADUATE SCHOOL
December 1986

Author:



Ioannis G. Vorrias

Approved by:



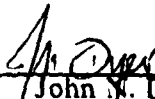
Richard W. Adler, Thesis Advisor



Harry Atwater, Second Reader



Harriett Rigas, Chairman,
Department of Electrical and Computer Engineering



John N. Dyer,
Dean of Science and Engineering

ABSTRACT

This thesis investigates the feasibility of two shipboard combat survivable HF communication antenna designs. Both antennas are modeled as a rectangular volume, which in one case is excited by a square patch atop a monopole, placed at various spacings from the center of one of the volume's faces, and in the other case is excited by a wire which is connected between the center of a face that is created by a rectangular shaped notch and a perfect ground plane. Several computer models of the two configurations for either different spacings between the patch monopole and the rectangular volume, or different notch sizes, are modeled with the Numerical Electromagnetics Code (NEC) and compared. Input impedances and radiation patterns of the two survivable antennas are presented. Both antennas are evaluated against a 3:1 Standing Wave Ratio (SWR) criterion.

RE: Report for Military Applications only/
Distribution Statement A is correct for this
report.

Per Professor Richard W. Adler, NPS/Code
62Ab



Accession For	
NTIS/DAI	<input checked="" type="checkbox"/>
DTIC	<input type="checkbox"/>
Unannounced	<input type="checkbox"/>
Justification	
By	
Distribution/	
Availability Codes	
Avail and/or	
Dist. Special	
A-1	

TABLE OF CONTENTS

I. INTRODUCTION 9
A. NEED FOR THE STUDY 9
B. STATEMENT OF THE PROBLEM 9
 1. Patch Monopole In Front Of The Box Configuration 10
 2. Notched Box Configuration 10
C. SCOPE AND LIMITATIONS 10

II. NUMERICAL COMPUTER MODELING 16
A. NUMERICAL ELECTROMAGNETICS CODE 16
B. MODELING GUIDELINES 20
 1. Wire Segment Modeling Guidelines 20
 2. Surface Patch Modeling Guidelines 21

III. COMPUTER MODELS - RESULTS 24
A. PATCH MONOPOLE IN FRONT OF THE BOX 24
B. NOTCHED BOX 46

IV. CONCLUSIONS AND RECOMMENDATIONS 65
A. CONCLUSIONS 65
B. RECOMMENDATIONS 66

APPENDIX : INPUT DATA SETS USED FOR THE MODELED ANTENNAS 68

LIST OF REFERENCES 75

BIBLIOGRAPHY 76

INITIAL DISTRIBUTION LIST 77

LIST OF TABLES

1. GRID DENSITY FOR THE PATCH MONOPOLE	27
2. SURFACE PATCH AREA FOR THE METAL BOX	28
3. AVERAGE GAIN AND INPUT IMPEDANCE VALUES	29
4. FREQUENCY RANGE SATISFYING A 3:1 SWR CRITERION	32
5. BOX NOTCHED BY A 4X2X12 METER VOLUME	48
6. BOX NOTCHED BY A 4X4X12 METER VOLUME	48
7. BOX NOTCHED BY A 4X6X12 METER VOLUME	49

LIST OF FIGURES

1.1	10x10 Meter Patch Monopole	11
1.2	Patch Monopole Centered in Front of the Box	12
1.3	12x12x12 Meter Box Notched by a 4x2x12 Meter Volume	13
1.4	12x12x12 Meter Box Notched By a 4x4x12 Meter Volume	14
1.5	12x12x12 Meter Box Notched by a 4x6x12 Meter Volume	15
2.1	Current Flow on a Surface	18
2.2	Induced Current by an Incident Wave	19
2.3	A Surface Patch	22
3.1	Patch Monopole Wire Grid Representation	25
3.2	Computer Model for the Patch Monopole in Front of the Box	26
3.3	Input Resistance vs Frequency for the Patch Monopole	30
3.4	Input Reactance vs Frequency for the Patch Monopole	31
3.5	Impedance Plot for 1.5 m Spacing Antenna Model	33
3.6	Impedance Plot for 2.0 m Spacing Antenna Model	34
3.7	Impedance Plot for 2.5 m Spacing Antenna Model	35
3.8	Smith Chart with 3:1 SWR Circle and Acceptable Region	36
3.9	Vertical Pattern (Height Near 0.1 Wavelength). $\Phi = 90^\circ$	37
3.10	Vertical Pattern (Height Near 0.1 Wavelength). $\Phi = 0^\circ$	38
3.11	Horizontal Pattern (Height Near 0.1 Wavelength)	39
3.12	Vertical Pattern (Height Near 0.2 Wavelength). $\Phi = 90^\circ$	40
3.13	Vertical Pattern (Height Near 0.2 Wavelength). $\Phi = 0^\circ$	41
3.14	Horizontal Pattern (Height Near 0.2 Wavelength)	42
3.15	Vertical Pattern (Height Near 0.4 Wavelength). $\Phi = 90^\circ$	43
3.16	Vertical Pattern (Height Near 0.4 Wavelength). $\Phi = 0^\circ$	44
3.17	Horizontal Pattern (Height Near 0.4 Wavelength)	45
3.18	Computer Model of the 4x4x12 m Notched Volume Box	47
3.19	Vertical Pattern for Range 2.0-3.0 MHz. $\Phi = 90^\circ$	50
3.20	Vertical Pattern for Range 2.0-3.0 MHz. $\Phi = 0^\circ$	51

3.21	Elevation Pattern for Range 2.0-3.0 MHz	52
3.22	Vertical Pattern for Range 3.0-4.0 MHz. $\Phi = 90^\circ$	53
3.23	Vertical Pattern for Range 3.0-4.0 MHz. $\Phi = 0^\circ$	54
3.24	Elevation Pattern for Range 3.0-4.0 MHz	55
3.25	Vertical Pattern for Range 6.0-7.5 MHz. $\Phi = 90^\circ$	56
3.26	Vertical Pattern for Range 6.0-7.5 MHz. $\Phi = 0^\circ$	57
3.27	Elevation Pattern for Range 6.0-7.5 MHz	58
3.28	Vertical Pattern for Range 7.5-9.0 MHz. $\Phi = 90^\circ$	59
3.29	Vertical Pattern for Range 7.5-9.0 MHz. $\Phi = 0^\circ$	60
3.30	Elevation Pattern for Range 7.5-9.0 MHz	61
3.31	Vertical Pattern for Range 9.0-10.0 MHz. $\Phi = 90^\circ$	62
3.32	Vertical Pattern for Range 9.0-10.0 MHz. $\Phi = 0^\circ$	63
3.33	Elevation Pattern for Range 9.0-10.0 MHz	64

ACKNOWLEDGEMENTS

I would like to express my thanks to Dr. Richard W. Adler, for his experienced guidance and warm assistance in this study.

I would also like to thank my wife Daisy, for relieving me of many family obligations during my studies, and especially during the research and development period of this thesis.

Finally I wish to thank all the Greek tax-payers, for having paid the expences of the period required for the completion of my course of studies.

I. INTRODUCTION

A. NEED FOR THE STUDY

The ability of a fighting ship to communicate with the rest of the world around it, in a considerable range, is one of the most important tasks, especially in a battle situation. Communication in different ranges for military applications, include UHF(Ultra High Frequency) communications, VHF(Very High Frequency) communications, and HF(High Frequency) communications.

UHF and VHF communications, due to short wavelengths, require small physical size antennas and a LOS (Line Of Sight) communication range. HF communications (2-30 MHz), due to long wavelengths, i.e. 150 meters for 2 MHz, require large antennas and can provide communication Over The Horizon (OTH).

Large physical size antennas, if they are composed of wires or whips with insulators at their bases, usually protrude from the ship's silhouette and are quite fragile and vulnerable to gun fire and bomb blast. The loss of a communications system can degrade the ship's fighting ability. Therefore, a study of methods which can make communication antennas more survivable is needed.

One approach to HF communications antenna design would be to excite sections of the ship's metal structure, allowing them to perform as antennas made as an integral part of the ship. For example, the ship's mast or stack might be excited and used as an antenna. Also the whole sub-structure of the bridge, the stern, or the bow, might be used to form, with proper excitation, an HF communications antenna. These and other possible survivable antenna designs, which can use patch or slot antennas or just coaxial feed lines for excitation, should be investigated.

B. STATEMENT OF THE PROBLEM

One possible antenna design would be to use a section of the ship's structure as an antenna. This study approximates a section of the ship's structure as a 12x12x12 meter metal box over a perfect ground (sea). The problem is to excite this metal box and determine the impedance and the radiation patterns of the antenna.

One way to excite a metal box, is to place close to it a conductive patch driven by a voltage or current source. Another way is using the same 12x12x12 meter hypothetical structure with a large notch, exciting it with a coaxial feed line connected between one of the notched faces and the perfect ground plane.

1. Patch Monopole In Front Of The Box Configuration

"Patch monopole" is the name chosen [Ref. 1: p.7], to describe the antenna used to excite the first possible antenna scheme. It is composed of a 10x10 meter patch atop a monopole 1 meter long. The size of the patch was chosen after the thorough investigation described in [Ref. 1: pages 68-71 and 104-122], where the 10x10 meter monopole was found to produce lower resistances and reactances than two other sizes, and most important, the computer model for the 10x10 meter patch monopole was found to be a close approximation to the real one which was constructed and tested for comparison with the computer model results. Figure 1.1 shows the patch monopole used for this study.

The patch monopole was centered in front of one of the metal box's faces with spacings varying from 1.5 meters to 2.5 meters. This range of appropriate spacings was selected after comparison of the values of the average gain resulting for different computer models. Figure 1.2 shows the patch monopole in front of the metal box.

2. Notched Box Configuration

The second possible scheme is a notched metal box of the same in size as the one used in the previous configuration. The notch's size was varied for testing purposes, in three sizes; 4x2x12, 4x4x12 and 4x6x12 meter; and different computer models were used for each size. The feed wire was connected as shown in Figures 1.3-1.5, between the upper notched face and the perfectly conducting ground. An E-gap voltage source was used to drive the center of the feed wire.

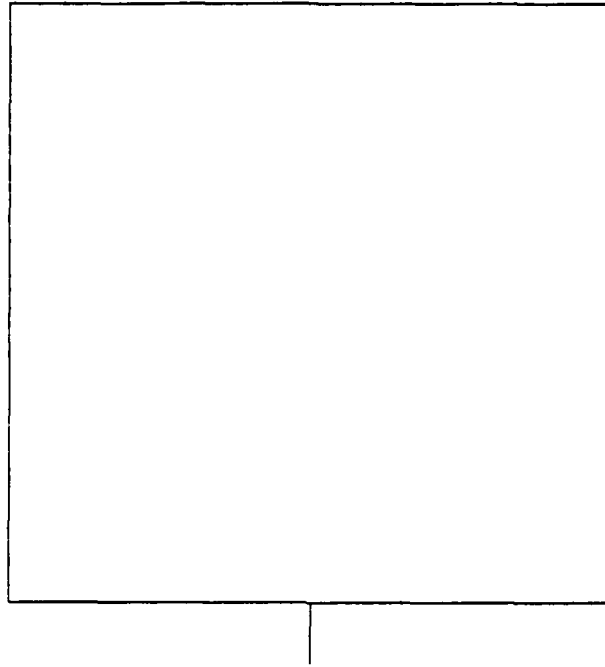


Figure 1.1 10x10 Meter Patch Monopole

C. SCOPE AND LIMITATIONS

This study concentrates on the results of using a patch monopole and different geometry schemes, properly connected with a feed line, to excite a rectangular volume.

The frequency range of the investigation is limited to 2-10 MHz. This limitation is imposed by computer storage and time restraints. As frequency increases, the wavelength decreases, and the object size in wavelengths increases. Sampling then is done on a minimum number of samples per wavelength.

The optimum computer modeling for the configuration of the patch monopole in front of the metal box and the configuration of the notched metal box, is a major emphasis of this study. The two antenna system surfaces are modeled using two different surface elements in the computer. A wire grid is

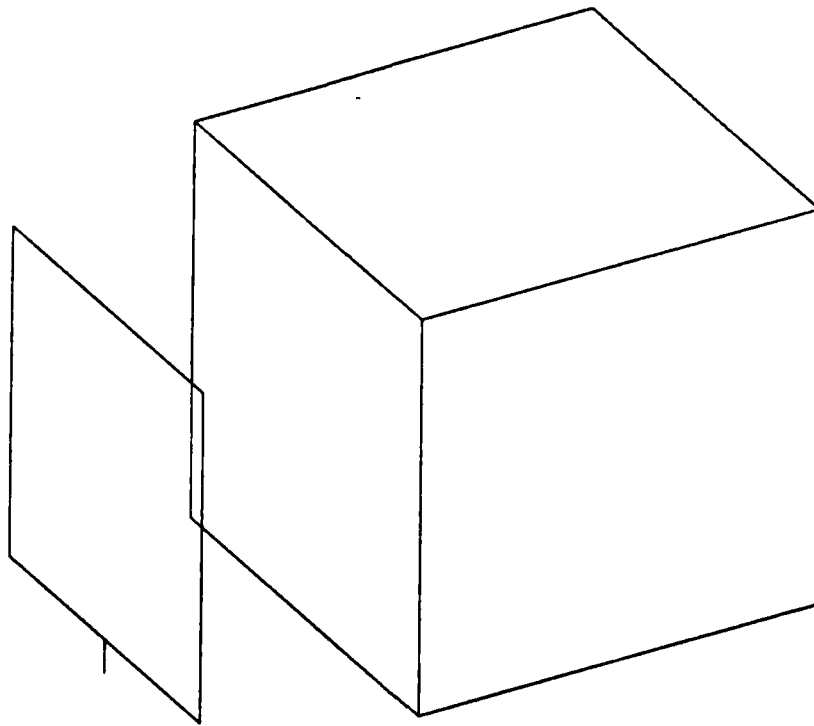
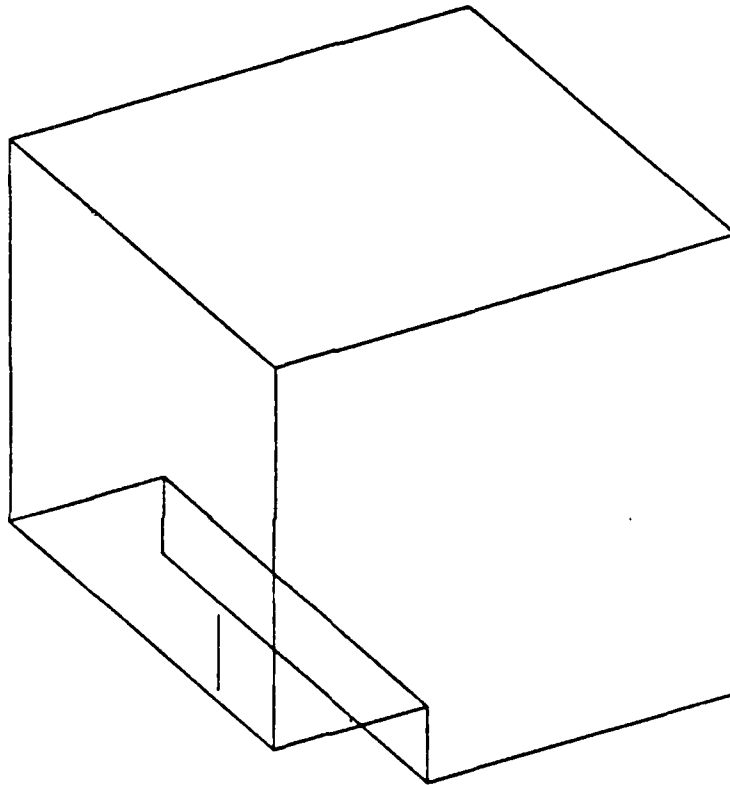


Figure 1.2 Patch Monopole Centered in Front of the Box

used to represent the patch monopole, and surface patches are used for the box structure. The computer code in this study is the Numerical Electromagnetics Code [Ref. 2].

This thesis starts with a discussion of computer antenna modeling in Chapter II. Chapter III describes the computer models developed for this study and presents the computed results, for which the conclusions and recommendations are presented in Chapter IV. Finally the Appendix contains sample computer data sets used in this study.

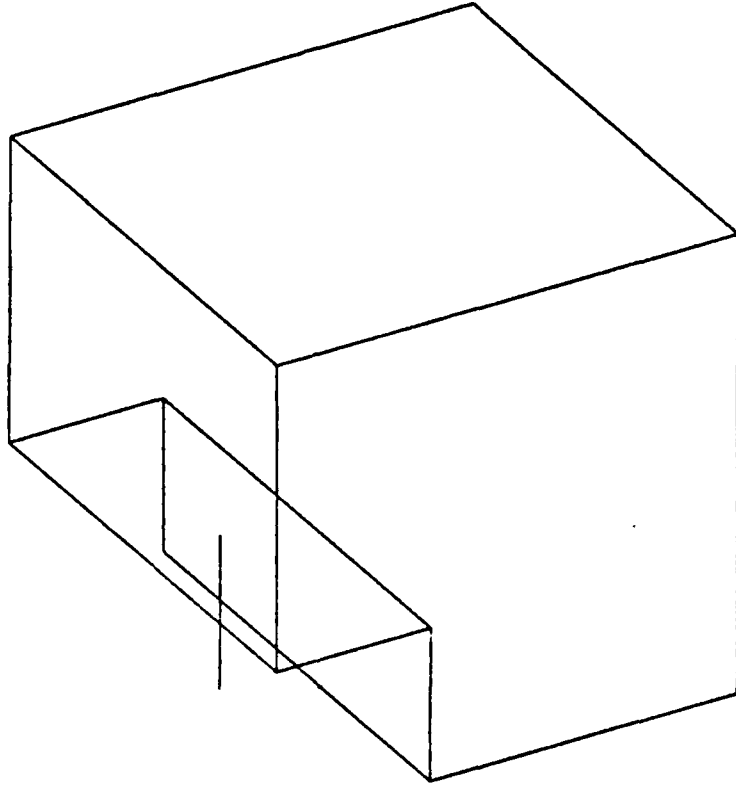
12X12X12 M BOX NOTCHED BY A 4X2X12 M VOLUME



THETA = 60.00 PHI = 60.00 ETA = 90.00

Figure 1.3 12x12x12 Meter Box Notched by a 4x2x12 Meter Volume

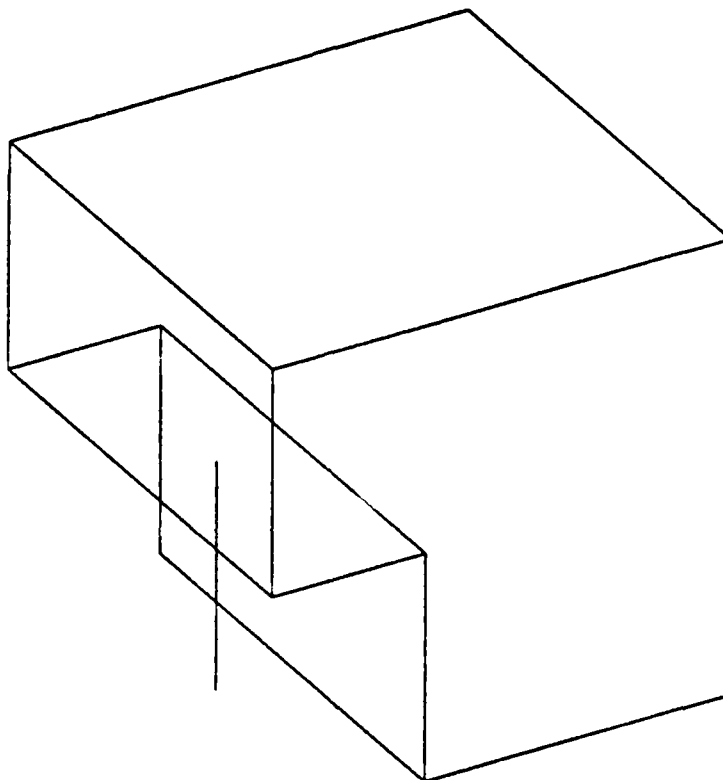
12X12X12 M BOX NOTCHED BY A 4X4X12 M VOLUME



THETA = 60.00 PHI = 60.00 ETA = 90.00

Figure 1.4 12x12x12 Meter Box Notched By a 4x4x12 Meter Volume

12X12X12 M BOX NOTCHED BY A 4X6X12 M VOLUME



THETA = 60.00 PHI = 60.00 ETA = 90.00

Figure 1.5 12x12x12 Meter Box Notched by a 4x6x12 Meter Volume

II. NUMERICAL COMPUTER MODELING

A. NUMERICAL ELECTROMAGNETICS CODE

The Numerical Electromagnetics Code, [Ref. 2], is a user oriented computer code, which has been developed at the Lawrence Livermore Laboratory, Livermore California, under the sponsorship of the Naval Ocean Systems Center and the Air Force Weapons Laboratory, for analyzing the electromagnetic response of an arbitrary structure consisting of thin wires and/or surface patches, over a ground plane or in free space. The arbitrary structure, can include either antennas or metal structures.

The code is built around the numerical solution of integral equations for induced currents on the structure. An incident plane wave or a source on a wire are the types of sources used for excitation of the structures. Structures are modeled using various geometry generation commands.

The code can provide outputs for current and charge density, electric or magnetic field in the vicinity of the structure, and radiated fields for plotting radiation patterns in any elevation and azimuth angle.

Convenient and accurate modeling of a wide range of structures is possible by proper combination of an integral equation for smooth surfaces with one for thin wires. One of the major features of NEC is the Numerical Green's Function for a partitioned-matrix solution, which allows efficient, repeated calculations for geometries where only a small portion of the structure changes. For obtaining accurate results the code requires a proper choice of either wire segment number or surface patches number, or both, to represent an antenna or other conducting surfaces in its vicinity, that affect its performance. As the structure's size is increased relative to wavelength, the numerical solution requires more computer time and file storage since the user must use a larger number of wire segments and/or surface patches for accuracy. One check for solution accuracy for a loss-free antenna is average gain value. The simplified formula for the average gain is given by equation 2.1:

$$G_{ave} = \kappa P_{rad} / P_{in} \quad , \quad (eqn 2.1)$$

where :

P_{rad} : radiated power which is integrated over a sphere
in the far-field

P_{in} : input power

κ : constant, which equals one for a structure in
free space and two for a structure over perfect
ground, for a loss-free antenna (radiated power
equals the input power).

Since in this study the two antenna configurations are considered lossless over perfect ground, the average gain for any input data should be close or equal to 2. Tables of the average gains for different frequencies, different notch sizes and different spacings between the patch monopole and the metal box are represented in Chapter III.

For a user to successfully use the code, he must understand the theory behind it. The electric field intensity $\bar{\mathbf{E}}$, due to an arbitrary known current, can be found (equation 2.2) by integrating the product of the free space Green's function and the known current density over the surface where the current flows, as shown in Figure 2.1.

$$\bar{\mathbf{E}}(\bar{\mathbf{r}}) = \int_S \bar{\mathbf{G}}(\bar{\mathbf{r}}, \bar{\mathbf{r}}') \bar{\mathbf{J}}_s(\bar{\mathbf{r}}') dA' \quad , \bar{\mathbf{r}} \in S \quad (\text{eqn 2.2})$$

When the current is unknown, an integral equation can be derived. When the electric field is evaluated for an observation point which lies on the surface S , then $\bar{\mathbf{E}}(\bar{\mathbf{r}})$ must satisfy the boundary condition:

$$\bar{\mathbf{n}} \times [\bar{\mathbf{E}}(\bar{\mathbf{r}}) + \bar{\mathbf{E}}^{\text{inc}}(\bar{\mathbf{r}})] = 0 \quad , \bar{\mathbf{r}} \in S \quad (\text{eqn 2.3})$$

Finally, as seen in [Ref. 3], the Electric Field Integral Equation (EFIE) becomes :

$$\bar{\mathbf{n}}(\bar{\mathbf{r}}) \times \int_S \bar{\mathbf{G}}(\bar{\mathbf{r}}, \bar{\mathbf{r}}') \bar{\mathbf{J}}_s(\bar{\mathbf{r}}') dA' = - \bar{\mathbf{n}}(\bar{\mathbf{r}}) \times \bar{\mathbf{E}}^{\text{inc}}(\bar{\mathbf{r}}) \quad , \bar{\mathbf{r}} \in S \quad , \quad (\text{eqn 2.4})$$

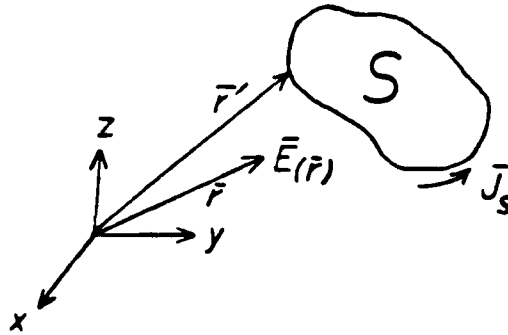


Figure 2.1 Current Flow on a Surface

where :

- $\bar{G}(\vec{r}, \vec{r}')$: Kernel
- $\bar{J}_s(\vec{r}')$: unknown
- $-\bar{n}(\vec{r}) \times \bar{E}^{inc}(\vec{r}')$: excitation function
- \int : principal value integral

The Magnetic Field Integral Equation (MFIE) has a different form and is expressed as follows :

$$1/2 \bar{J}_s(\vec{r}) + 1/4\pi \int_S \bar{n}(\vec{r}) \times \bar{J}_s(\vec{r}') \times \nabla' g(\vec{r}, \vec{r}') = -\bar{n}(\vec{r}) \times \bar{H}^{inc}(\vec{r}) , \quad (\text{eqn 2.5})$$

where $\bar{J}_s(\vec{r})$ is again unknown.

NEC uses the EFIE for wire structures and the MFIE for surface patches.

When a perfectly conducting ground is present, the current is induced on the ground plane as well on the surface \$S\$ as shown in Figure 2.2.

In this case, the integral equation is derived from the free-space Green's function, and has the form :

$$\bar{n} \times \int_{S+S_{(pg)}} \bar{G}(\vec{r}, \vec{r}') \bar{J}(\vec{r}') dA' = -\bar{n} \times \bar{E}_{inc}(\vec{r}) , \quad \vec{r} \in S+S_{(pg)} \quad (\text{eqn 2.6})$$

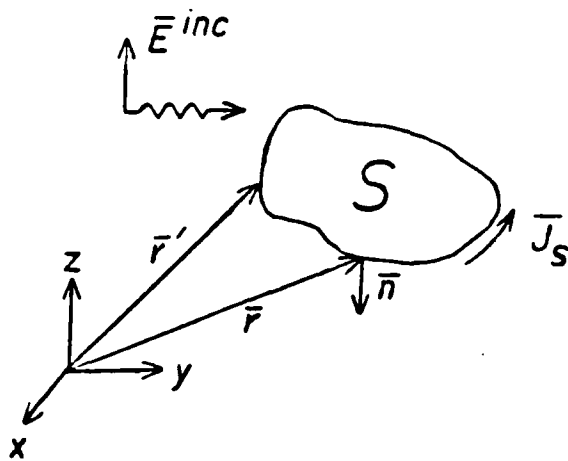


Figure 2.2 Induced Current by an Incident Wave

Since the perfect ground extends to infinity, the above equation is not easily solved. The solution is achieved using the Method of Moments (MoM), [Ref. 4], where the current is expanded in a set of N basis functions. $\bar{J}_s(\bar{r}') = \sum a_n \bar{j}_n(\bar{r}')$ and the integral equation becomes:

$$\sum_{n=1}^N a_n M[\bar{j}_n(\bar{r}')] = \bar{F}(\bar{r}), \tag{eqn 2.7}$$

where M is a linear operator. The inner product is then taken with a set of N weight functions $W_m, m = 1, \dots, N$:

$$\sum_{n=1}^N a_n \langle W_m(\bar{r}'), M[\bar{j}_n(\bar{r}')] \rangle = \langle W_m(\bar{r}'), \bar{F}(\bar{r}') \rangle, \tag{eqn 2.8}$$

which is equivalent to:

$$\sum_{n=1}^N I_n x z_{nm} = V_m, \quad m = 1, \dots, N \tag{eqn 2.9}$$

The weight functions in NEC are Dirac delta functions at the centers of wire segments. The weighting functions have the form :

$$M_m(r) = \delta(S - S_m) , \quad (\text{eqn 2.10})$$

where S_m are the set of the match points found at the center of each segment S .

For thin wires for which the wire radius is small compared to a wavelength, the integral equation is reduced to a scalar equation and the basis functions provide a continuous current and charge density. It is important for the user to know that the selection of the basis functions and the weighting functions affects the accuracy of the solution and the efficiency of the computation. This translates into users being required to carefully develop computer models and to intimately know the limitations of the code.

Having approximate the current distribution over an arbitrary structure, the antenna's input impedance, gain, efficiency, radiation patterns, currents, charge distribution, coupling, near field values, and polarization can be easily calculated as needed.

B. MODELING GUIDELINES

1. Wire Segment Modeling Guidelines

Wire segments are modeled in NEC such that both geometric and electrical factors are involved. Segments which are defined by coordinates of their end points and their radius, should follow the paths of conductors as closely as possible. Only axial currents are considered and there is no allowance for circumferential variation of the current. The accuracy of the mathematical solution depends on a many constraints which form the following electrical considerations for single wire segments or wire grid models of conducting surfaces:

- (a) The segment length Δ relative to a wavelength λ is a key parameter :
 - Δ should be less than $.1\lambda$ for accurate results in most cases.
 - Δ should be less than $.05\lambda$ in critical regions.
 - Δ could be less than $.2\lambda$ on long, straight segments.
 - Δ should not be less than $10^{-4} \lambda$

- (b) The radius α should be small relative to both λ and Δ :
 - α should be less than $.5\Delta$
 - α should be less than $.1\lambda$
- (c) The user should avoid large radius changes if it is needed, especially in short segments, and also avoid sharp bends in thick segments.
- (d) Wires that are connected must contact at segment ends. If the separation of two segment ends is less than 10^{-3} times the length of the shortest segment, then they are considered as connected.
- (e) Segments before and after the segment on which a voltage source is applied should be equal in length and radius. When the source is at the base of a segment connected to a ground plane, then this segment should be vertical.
- (f) The more segments used in a wire grid to model a solid structure, the more accurate the solution due to the avoidance of high inductances normally present in sparse grids.

2. Surface Patch Modeling Guidelines

NEC includes a patch option for modeling closed surfaces with non vanishing enclosed volume, using the Magnetic Field Integral Equation.

The model is constructed with multiple, small flat surface patches. These correspond to wire segment cells that are used to model surfaces as wire grids.

A surface patch is defined by its area, the coordinates of the center, and the components of the outward directed unit normal vector (Figure 2.3).

The position of the patch's center is determined by the equation : $\bar{r}_0 = x_0 \hat{x} + y_0 \hat{y} + z_0 \hat{z}$, and the outward directed normal unit vector is defined by : $\hat{n} = n_x \hat{x} + n_y \hat{y} + n_z \hat{z}$. The code computes the surface current on each patch along the orthogonal unit vectors \hat{t}_1 and \hat{t}_2 which are tangent to the surface of the patch.

When a rectangle is divided into patches, the direction of the outward normals \hat{n} of the patches are determined by the ordering of its corner coordinates and the right hand rule. When \hat{t}_1 is specified by the geometry, then $\hat{t}_2 = \hat{n} \times \hat{t}_1$.

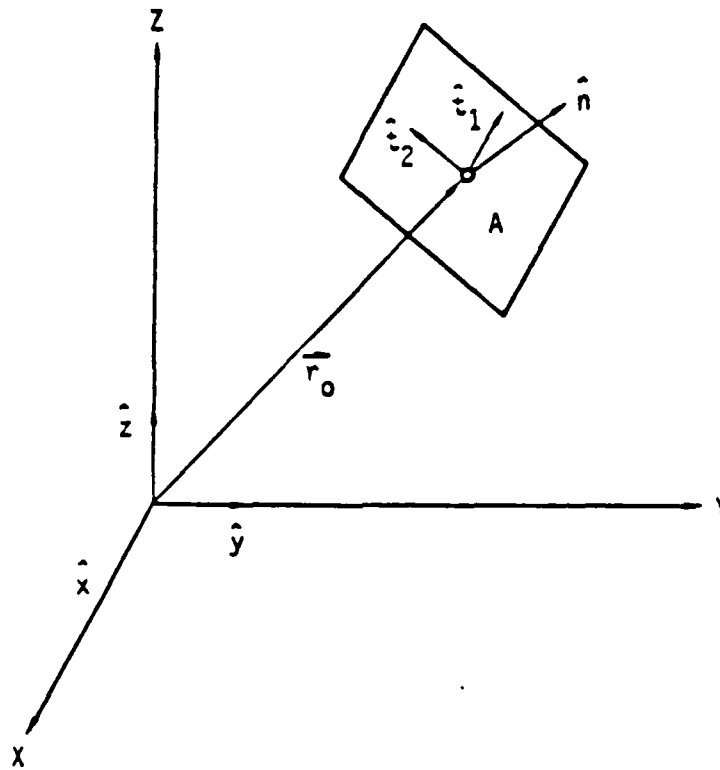


Figure 2.3 A Surface Patch

The connection of a wire segment with a surface patch requires that the wire must end at the center of the patch, with identical coordinates used for the wire end and the patch center. The code then divides the connected patch into four equal patches about the wire end. The division of the connected patch is along lines defined by the vectors \hat{t}_1 and \hat{t}_2 . NEC, by computing the interactions between these four patches and the lowest segment on the connecting wire, applies an interpolation function on them, to represent the current from the wire onto the surface, and that function is numerically integrated over the patches. Connected patches should be approximately square, with sides parallel to \hat{t}_1 and \hat{t}_2 . The connected wire cannot lie in the plane of the patch, but it is not required to be normal to the patch. Also, a wire may never be connected to a patch which has been previously divided.

For accurate results, the following guidelines apply :

- (a) The area of an individual surface patch should be less than $.04\lambda^2$ ($.2\lambda \times .2\lambda$).
- (b) The number of patches used to model a surface should be greater than 25 per square wavelength.
- (c) Even though there is no restriction in following a specific shape of patches, avoid long, thin patches.
- (d) Where the radius of curvature is small, the user can use smaller patches.
- (e) The modelled surface must be closed and not too thin (no plates, no fins, no wings).
- (f) A large patch may be used for a connection with a wire segment to anticipate the subdivision into four smaller patches.

III. COMPUTER MODELS - RESULTS

In this section of the study, computer models used for the two design configurations of survivable antennas are described. Also the computed results for average gain, input impedance, Standing Wave Ratio (SWR), and radiation patterns are presented.

Frequency stepping for 2-10 Mhz was multiplicative, with a multiplication factor (MF) of 1.2228445, computed using [Ref. 2: p. 59], the following formula:

(eqn 3.1)

$$MF = \sqrt[n-1]{f_{hi} / f_{lo}} \quad , n = \text{Number of Frequencies}$$

The average gain value, as an indication of a numerically stable model, can provide a check on the accuracy of the computed input impedance over a perfect ground plane, and as mentioned in Chapter II it should equal the value of two.

A. PATCH MONOPOLE IN FRONT OF THE BOX

The patch monopole, as discussed in Chapter I, is a 10x10 m patch atop a one meter monopole. The surface of the patch was modeled as a wire grid, with grid spacing of one meter, as shown in Figure 3.1. 220 wire segments were used to represent the patch's surface. The feed monopole was modeled with one wire segment as was determined by [Ref. 1], where the one segment feed line provided good results, probably due to the fact that the same segment length of one meter is used for the patch wire grid to which it is connected.

The 12x12x12 meter box, was modeled in NEC with surface patches. The area of each patch was selected to be 2x2 meters.

An attempt to model both the patch monopole and the metal box by a more dense wire grid and smaller patch area for higher accuracy, was impactful due to excessive computer processing time. Figure 3.2 shows the computer model representation that was used for this configuration.

PATCH ANTENNA ATOP A MONOPOLE (WIRE GRID REPRESENTATION)

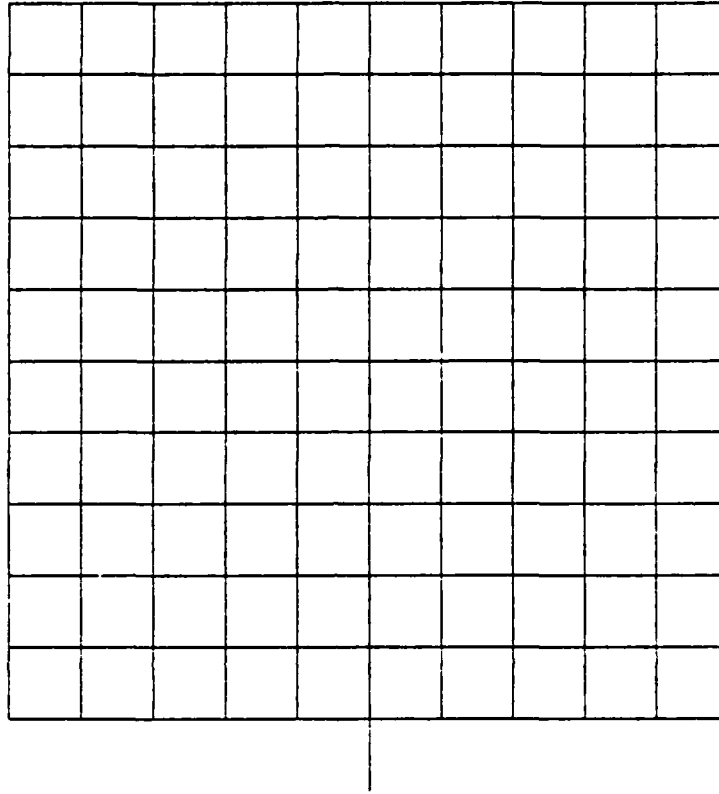
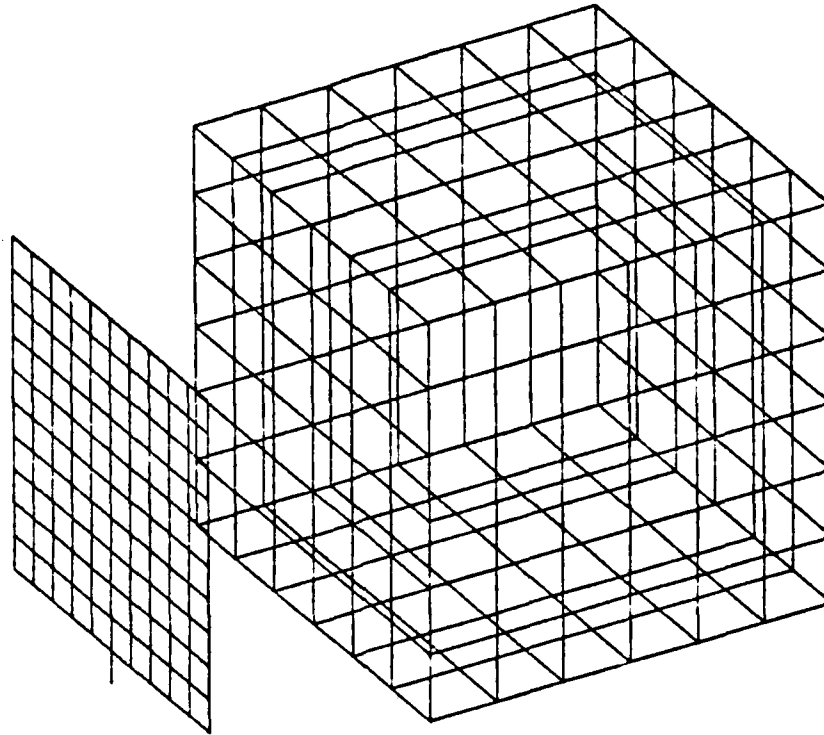


Figure 3.1 Patch Monopole Wire Grid Representation

Table 1 provides the patch monopole grid density in wavelengths. Table 2 provides the surface patch area in square wavelengths for the metal box.

The average gain values and input impedance values for varying spacing of the patch monopole from the box, and for frequencies chosen via multiplicative stepping, are presented in Table 3 . Figures 3.3 and 3.4 are the plots of the input resistance and input reactance versus frequency for the three models of the survivable communications antenna.

In Table 3, it is seen that the average gain values are not all as desired, ie. close to the value of two. The fact that as the spacing of the patch monopole



$$\text{THETA} = 60.00 \quad \text{PHI} = 60.00 \quad \text{ETA} = 90.00$$

Figure 3.2 Computer Model for the Patch Monopole in Front of the Box

from the box increases, the average gain approaches the ideal value of 2, does not mean wide patch monopole - box spacing is better. It is evident that as the spacing of the patch monopole from the box increases, the metal box has less effect on the pattern of the combination, until the results will depend only upon the patch monopole itself. That was the reason that the test spacings of the patch monopole from the box were kept in the region of 1.5 to 2.5 meters, even though the average gain values may have improved as the distance was increased.

TABLE I
GRID DENSITY FOR THE PATCH MONOPOLE

Frequency (MHz)	Wavelength (m)	Grid Density in Wavelengths
2.00	150.0	0.00667
2.44	122.7	0.00815
2.99	100.4	0.00997
3.65	82.0	0.0121
4.47	67.0	0.0149
5.46	54.8	0.0182
6.68	44.8	0.0223
8.17	36.7	0.0272
10.00	30.0	0.0333

The NEC computer models of the patch monopole in front of the box were all fed with an E-gap voltage source placed at the base of the feed segment. Placing the voltage source at the segment touching the ground is equivalent to placing it at the center of two antennas (the actual one and the mirror image), and does not violate the modeling guideline of having equal length segments on either side of a voltage source. For the test frequency range of 2-10 MHz, the entire configuration even if it is physically large in size, corresponds to small electrical heights, which vary from 0.08λ for 2 MHz to 0.4λ for 10 MHz. This fact was expected to have an effect on the input impedance values, especially for the lower region of the frequency range. Input resistances are very small for low frequencies, where the electrical height is very small. Also the input reactance values are capacitive for low frequencies and inductive for higher frequencies, as expected.

Smith chart plots of the impedance characteristics for the spacings from 1.5 meters to 2.5 meters are presented in Figures 3.5 through 3.7. For this study, a SWR of 3:1 was considered as a reasonable criterion for practical operation.

TABLE 2
SURFACE PATCH AREA FOR THE METAL BOX

Frequency (MHz)	Square Wavelength (m ²)	Area In Sq. Wavelength
2.00	22,470.01	0.000178
2.44	15,030.76	0.000268
2.99	10,060.09	0.000397
3.65	6,725.64	0.000594
4.47	4,494.36	0.000891
5.46	3,006.32	0.00133
6.68	2,010.62	0.00198
8.17	1,344.68	0.00297
10.00	898.80	0.00445

Even though not many antennas satisfy this criterion over an operating band of frequencies, many of them can be brought into this region of the Smith chart by the use of series inductance or capacitance [Ref. 5]. Figure 3.8 presents the 3:1 SWR circle. The shaded region presents the impedance region of the Smith chart which may be moved into the 3:1 SWR by the use of series reactances. Any impedance that falls in the 3:1 SWR circle or in the shaded region of the Smith chart, will be considered as acceptable.

The frequency range for various spacings of the patch monopole from the box, that fall in the previous mentioned regions of the Smith chart, are presented in Table 4 .

As it can be seen from the Smith chart plots, and Table 4, the range of frequencies satisfying the 3:1 SWR is limited in the higher region of the test frequency range.

Radiation patterns were obtained for three model configurations ie. for 1.5, 2.0, and 2.5 meter monopole-box spacing. The large size of the box compared to the size of the patch monopole, and the small variation of spacing

TABLE 3
AVERAGE GAIN AND INPUT IMPEDANCE VALUES

PATCH MONOPOLE IN FRONT OF THE BOX CONFIGURATION

Frequency (MHz)	Spacing From Box (m)	Average Gain	Input Impedance (Ohms) $r + jx$
2.00	1.5	1.51	0.120 - j61.7
	2.0	1.69	0.190 - j68.7
	2.5	1.78	0.271 - j75.9
2.44	1.5	1.65	0.183 - j41.6
	2.0	1.67	0.325 - j44.5
	2.5	1.75	0.458 - j50.0
2.99	1.5	1.66	0.249 - j23.0
	2.0	1.68	0.453 - j26.0
	2.5	1.72	0.637 - j30.0
3.65	1.5	1.75	0.225 - j4.68
	2.0	1.77	0.367 - j6.59
	2.5	1.79	0.534 - j8.99
4.47	1.5	2.09	0.212 + j15.4
	2.0	2.06	0.414 + j14.8
	2.5	2.03	0.637 + j13.5
5.46	1.5	2.07	0.681 + j45.5
	2.0	2.05	1.75 + j49.7
	2.5	2.02	2.25 + j44.8
6.68	1.5	2.06	1.34 + j29.9
	2.0	2.04	2.67 + j31.5
	2.5	2.01	3.31 + j50.6
8.17	1.5	2.05	5.35 + j75.0
	2.0	2.02	12.8 + j66.5
	2.5	2.01	26.1 + j80.4
10.0	1.5	2.04	32.4 + j142.4
	2.0	2.01	84.0 + j165.1
	2.5	2.01	146.5 + j143.4

between the patch monopole and the box compared to wavelength were the reasons that the patterns of the three modeled configurations were almost identical. For frequencies where the the antenna's height is less than a tenth of a wavelength, the patterns are similar to those of an electrically short monopole. For higher frequencies, where the antenna's height becomes near two tenths of a

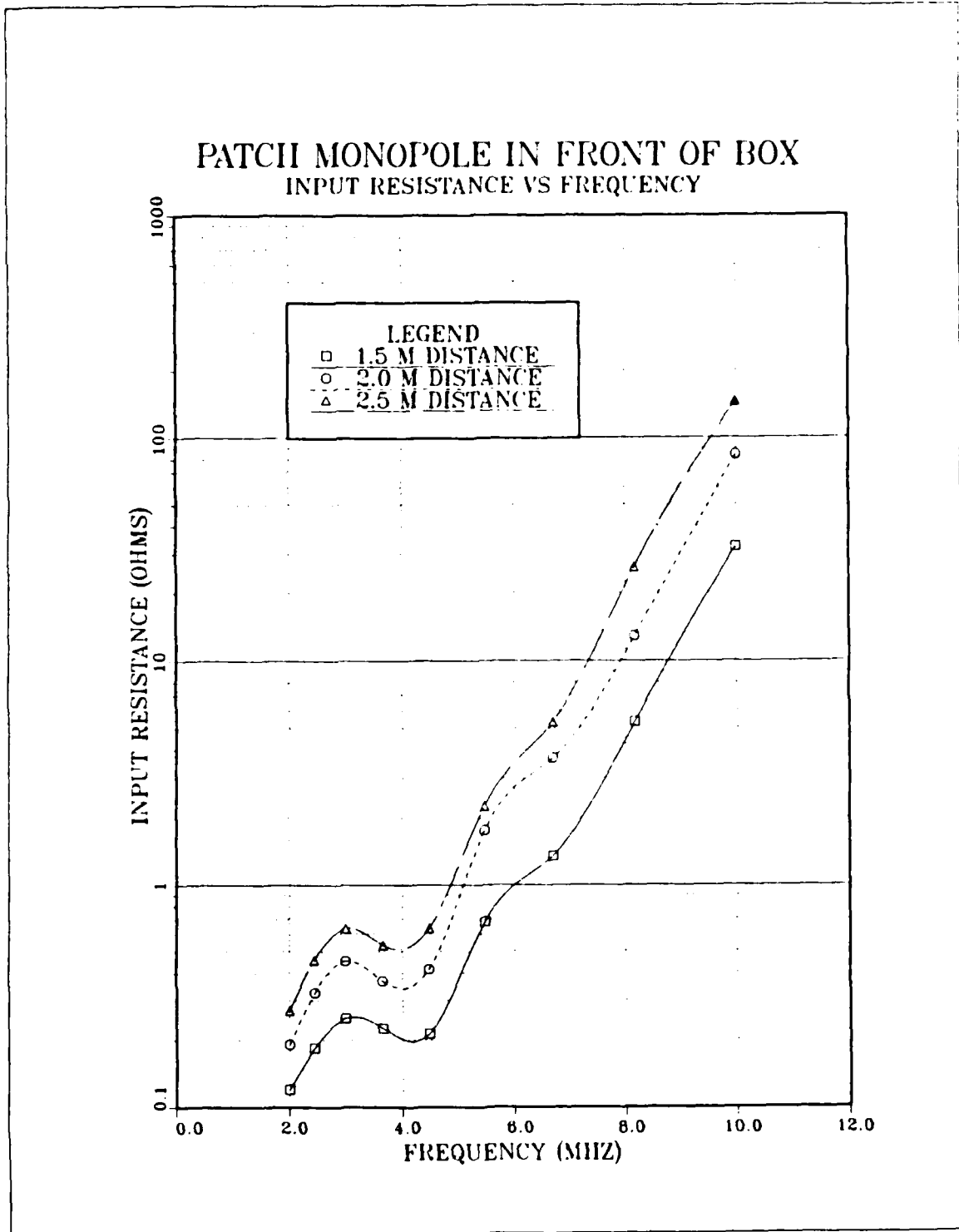


Figure 3.3 Input Resistance vs Frequency for the Patch Monopole

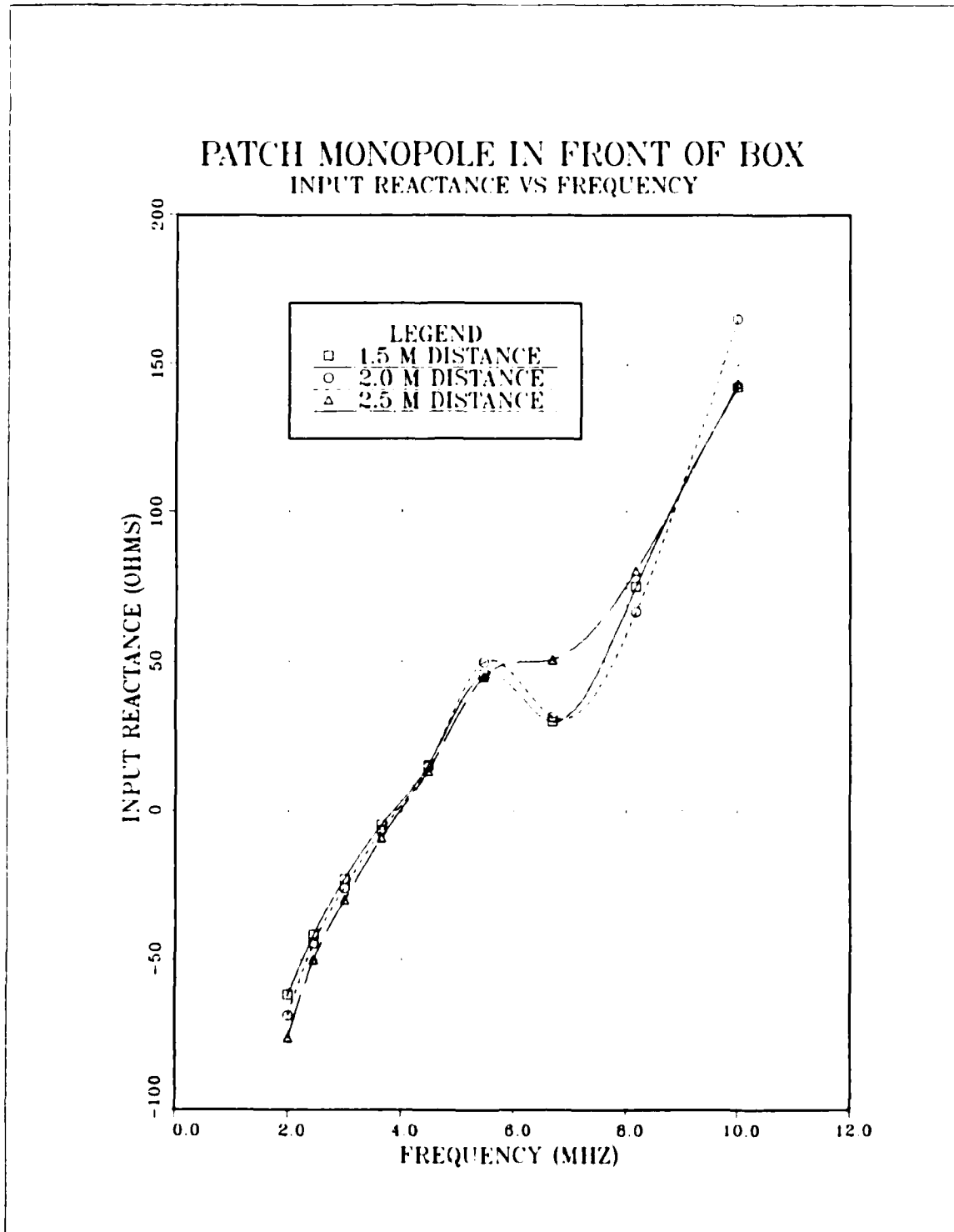


Figure 3.4 Input Reactance vs Frequency for the Patch Monopole

TABLE 4
FREQUENCY RANGE SATISFYING A 3:1 SWR CRITERION

DISTANCE FROM BOX (m):	1.5	2.0	2.5
FREQUENCY RANGE (MHz):	8.5 - 10.0	8.0 - 10.0	7.5 - 10.0

wavelength, the patterns are more uniform, although they are "compressed" at the sides of the box. Figures 3.12-3.14 are typical of these patterns.

As the antenna's height approaches a fourth of a wavelength, the horizontal patterns become more directional at the monopole face of the box, and the gain is decreased on the opposite side. The vertical patterns are similar to those of an equal-sized monopole, but are stretched at the side of the box opposite to the monopole. The patterns are also less strongly lobed than the vertical patterns of an equal-sized monopole since the intense null at the 90 degree elevation angle no longer exists. Figures 3.15- 3.17 show these properties. Finally, the gain is greater for higher elevation angles, compared with the gain of a monopole with equal height, a useful condition for Near Vertical Incidence (NVIS) ionospheric communication paths.

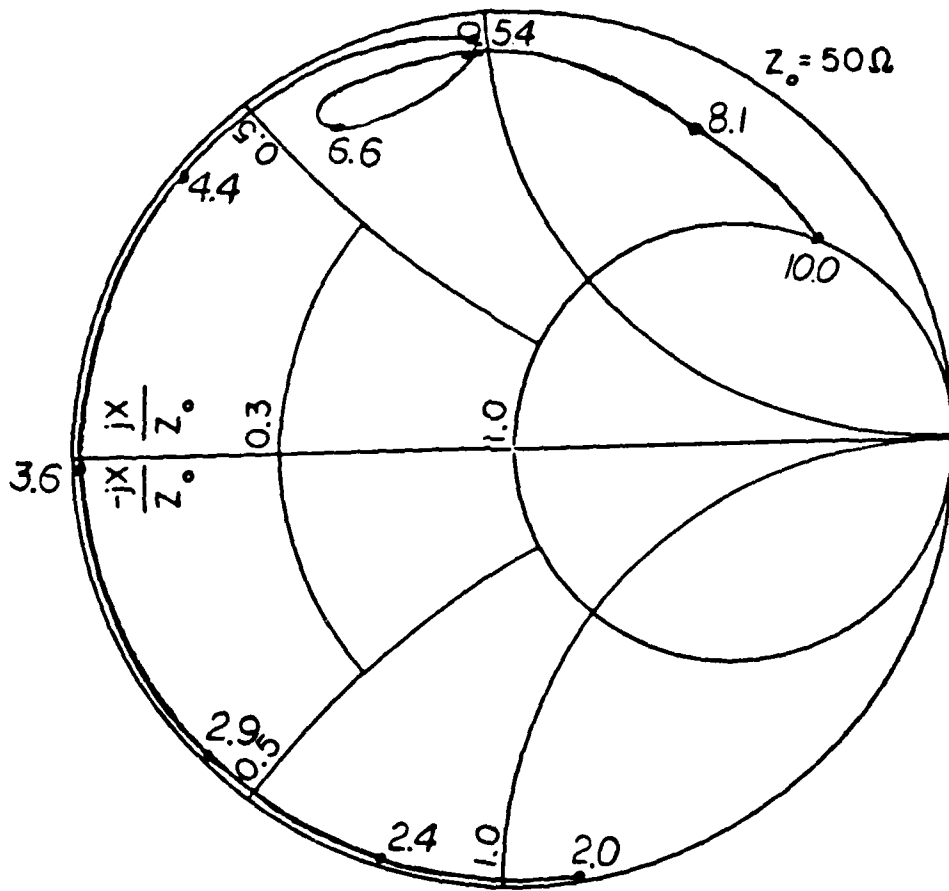


Figure 3.5 Impedance Plot for 1.5 m Spacing Antenna Model

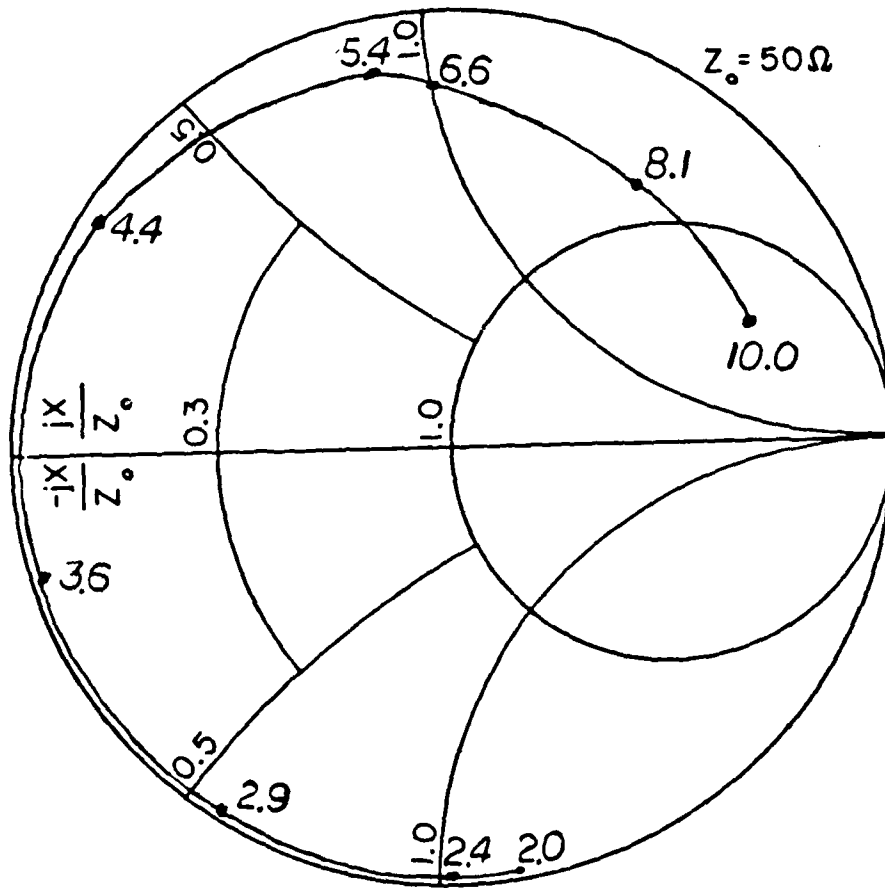


Figure 3.7 Impedance Plot for 2.5 m Spacing Antenna Model

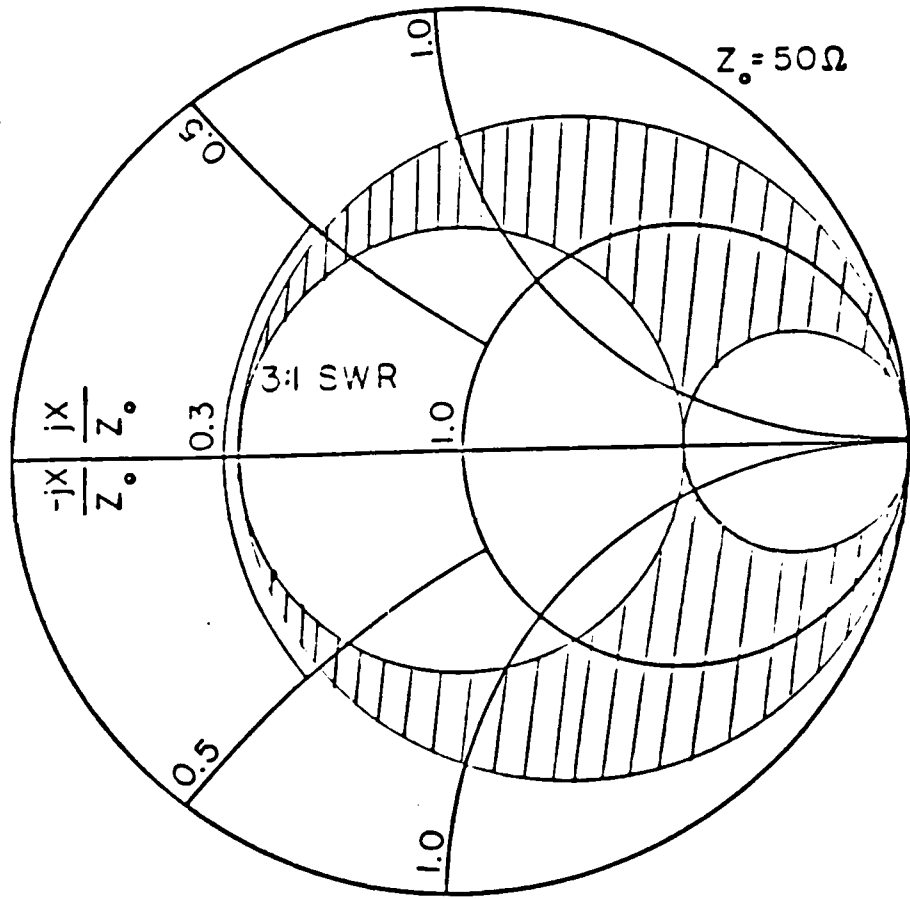


Figure 3.8 Smith Chart with 3:1 SWR Circle and Acceptable Region

PATCH MONOPOLE AT DISTANCE 1.5 M FROM THE BOX. FREQ = 2 MHZ

VERTICAL PATTERN (YZ PLANE), AZIMUTH ANGLE = 90 DEG.

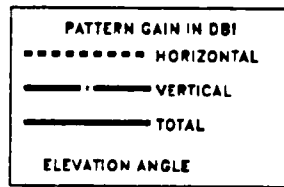
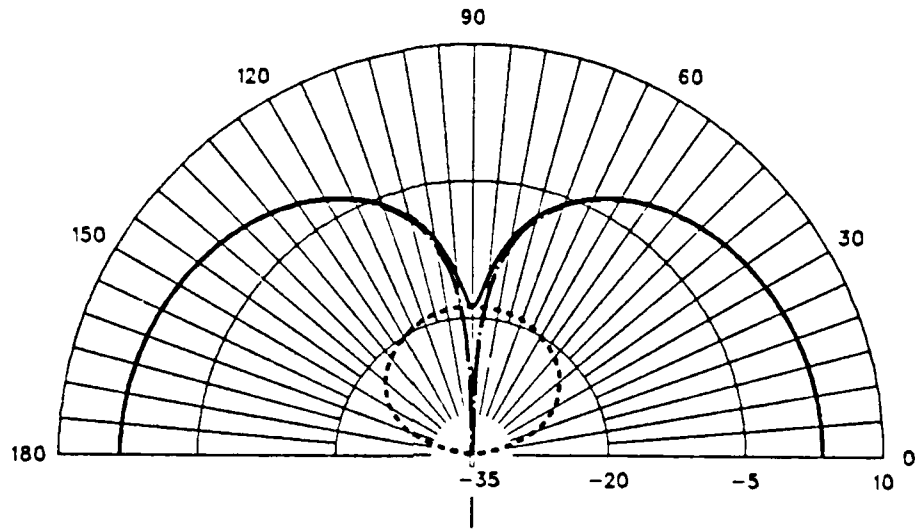


Figure 3.9 Vertical Pattern (Height Near 0.1 Wavelength). $\Phi = 90^\circ$

PATCH MONOPOLE AT DISTANCE 1.5 M FROM THE BOX. FREQ = 2 MHZ

VERTICAL PATTERN (XZ PLANE), AZIMUTH ANGLE = 0 DEG.

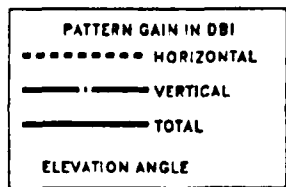
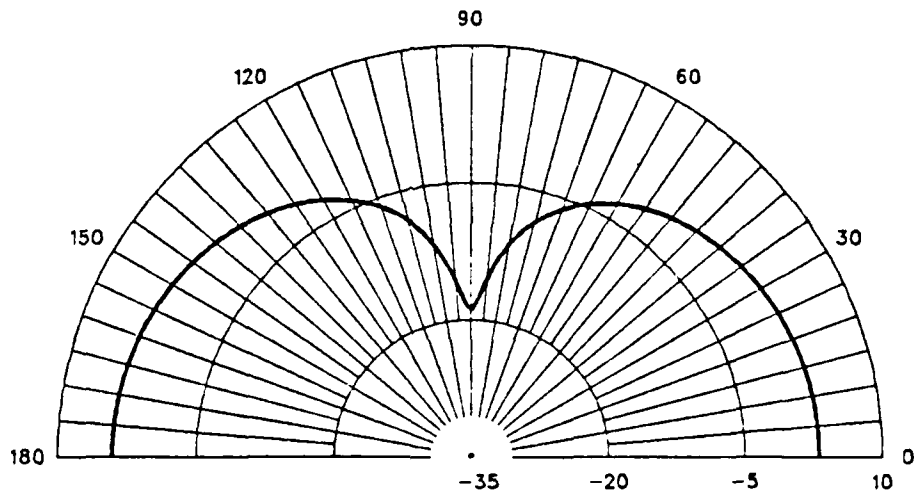


Figure 3.10 Vertical Pattern (Height Near 0.1 Wavelength). $\Phi = 0^\circ$

PATCH MONOPOLE AT DISTANCE 1.5 M FROM THE BOX. FREQ = 2 MHZ

AZIMUTH PATTERN (XY PLANE), ELEVATION ANGLE = 30 DEG.

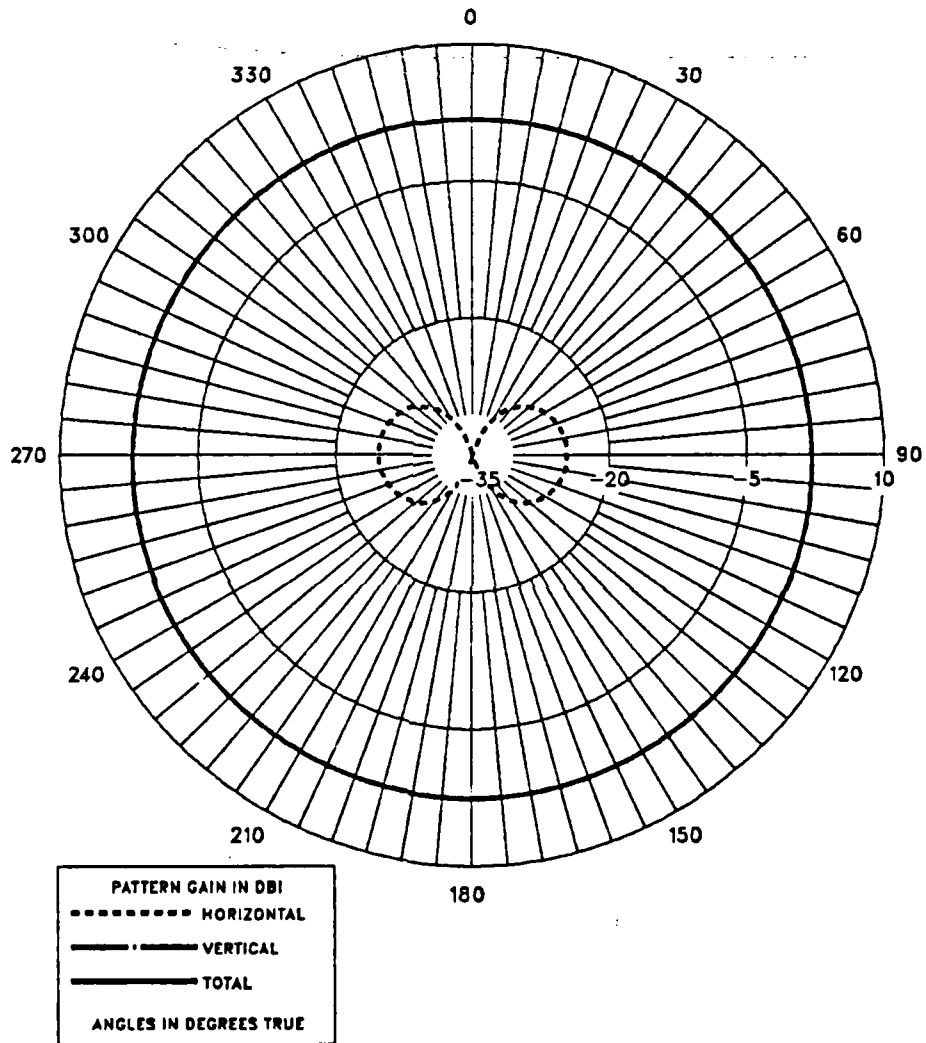


Figure 3.11 Horizontal Pattern (Height Near 0.1 Wavelength)

PATCH MONOPOLE AT DISTANCE 2 M FROM THE BOX. FREQ=4.4MHZ

VERTICAL PATTERN(YZ PLANE), AZIMUTH ANGLE = 90 DEG.

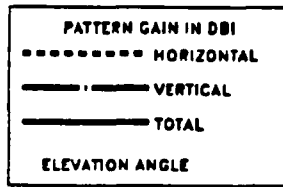
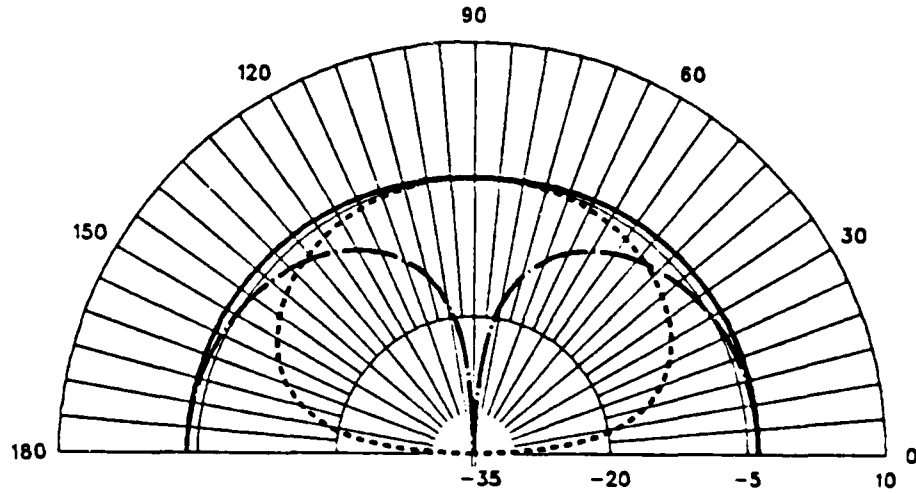


Figure 3.12 Vertical Pattern (Height Near 0.2 Wavelength). $\Phi = 90^\circ$

PATCH MONOPOLE AT DISTANCE 2 M FROM THE BOX. FREQ=4.4MHZ

VERTICAL PATTERN (XZ PLANE), AZIMUTH ANGLE = 0 DEG.

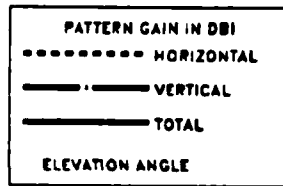
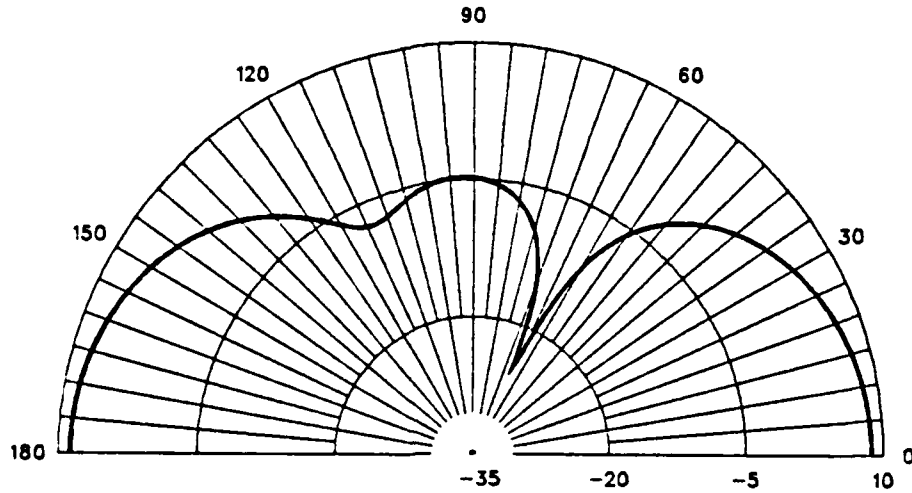


Figure 3.13 Vertical Pattern (Height Near 0.2 Wavelength). $\Phi = 0^\circ$

PATCH MONOPOLE AT DISTANCE 2 M FROM THE BOX, FREQ=4.4MHZ

AZIMUTH PATTERN (XY PLANE), ELEVATION ANGLE = 30 DEG.

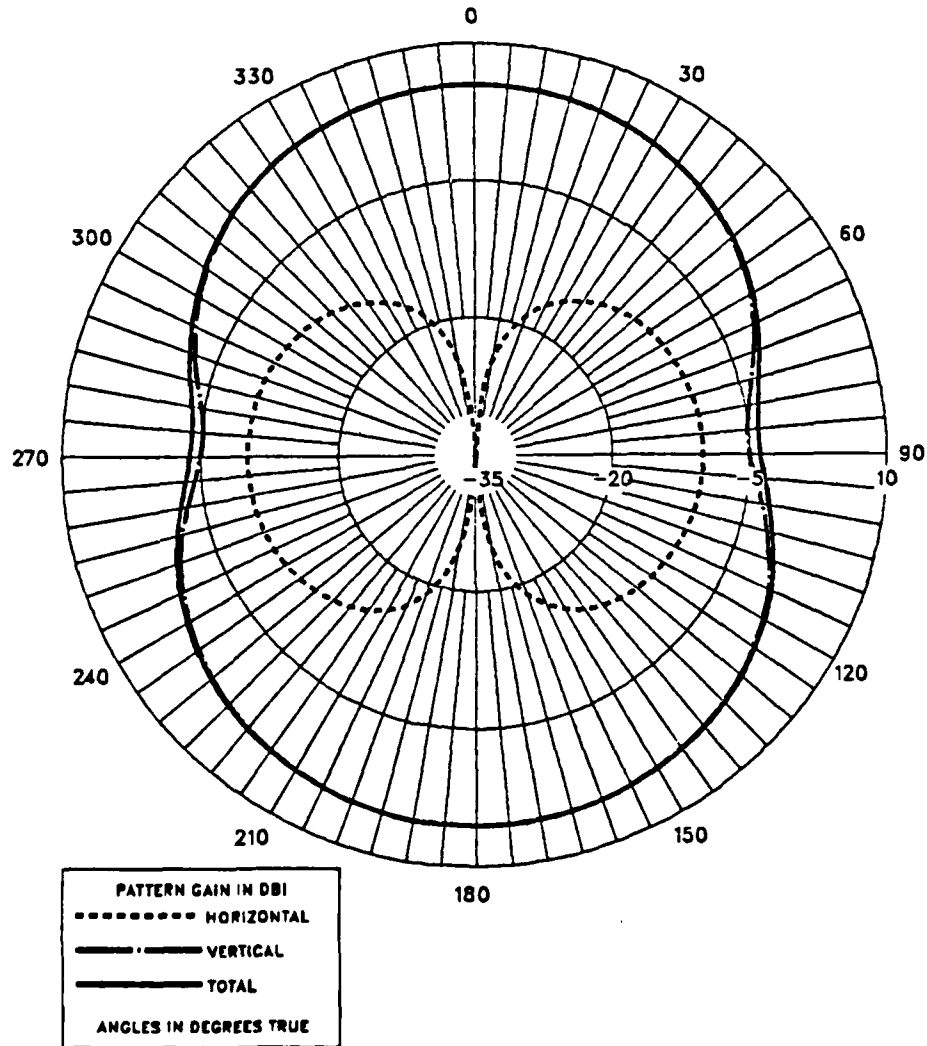


Figure 3.14 Horizontal Pattern (Height Near 0.2 Wavelength)

PATCH MONOPOLE AT DISTANCE 2.5 M FROM THE BOX. FREQ= 10 MHZ

VERTICAL PATTERN (YZ PLANE), AZIMUTH ANGLE = 90 DEG.

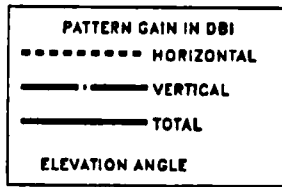
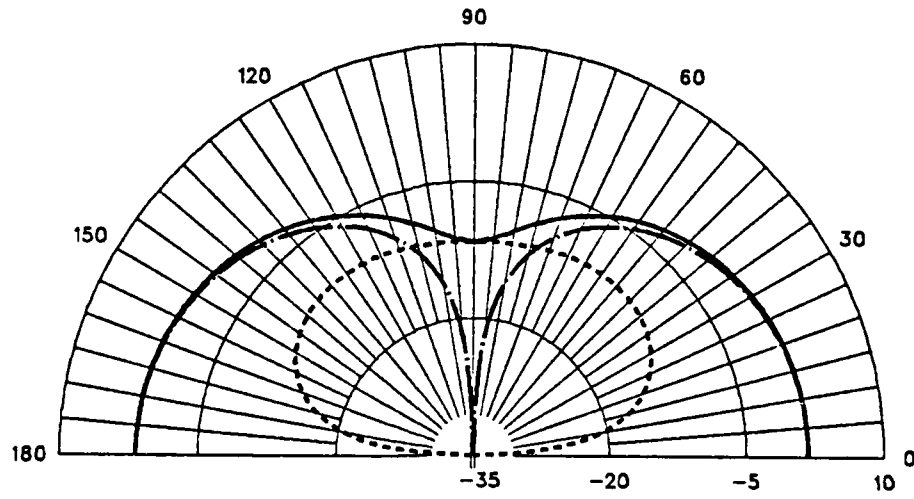


Figure 3.15 Vertical Pattern (Height Near 0.4 λ Wavelength). $\Phi = 90^\circ$

PATCH MONOPOLE AT DISTANCE 2.5 M FROM THE BOX. FREQ= 10 MHZ

VERTICAL PATTERN (XZ PLANE), AZIMUTH ANGLE = 0 DEG.

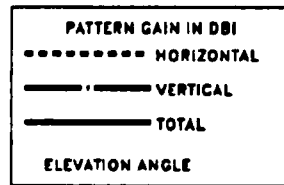
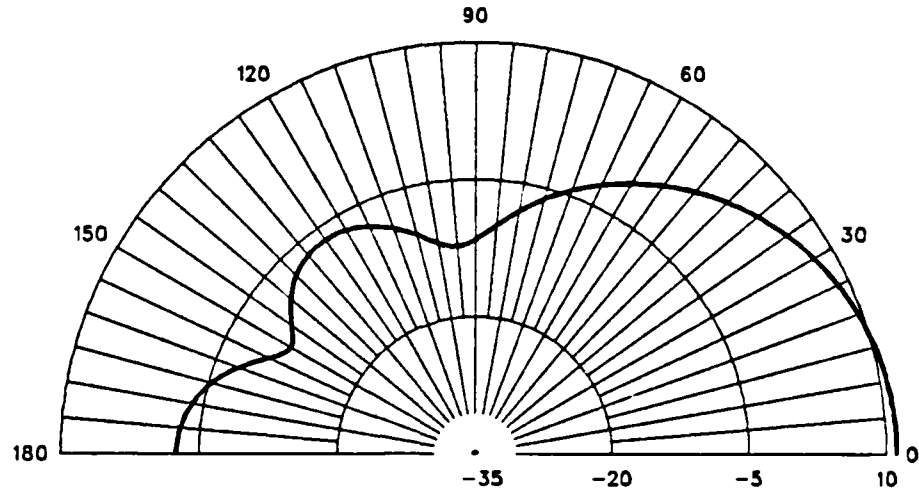


Figure 3.16 Vertical Pattern (Height Near 0.4 Wavelength). $\Phi = 0^\circ$

PATCH MONOPOLE AT DISTANCE 2.5 M FROM THE BOX. FREQ= 10 MHZ

AZIMUTH PATTERN (XY PLANE), ELEVATION ANGLE = 30 DEG.

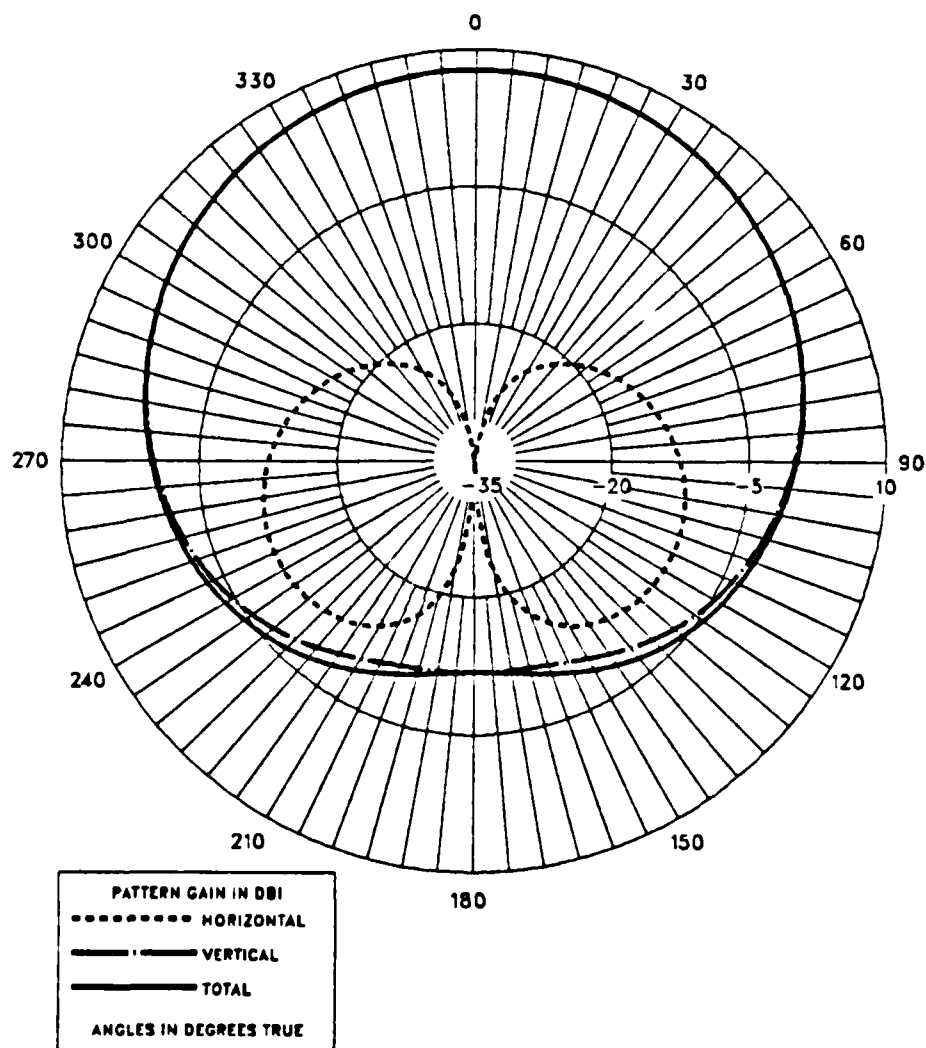


Figure 3.17 Horizontal Pattern (Height Near 0.4 Wavelength)

B. NOTCHED BOX

As discussed in Chapter I, three versions of the notched box configuration were tested with NEC. All three of them differ in the notched volume size, which was varied as 4x2x12, 4x4x12, and 4x6x12 meters. All surfaces of the three models were represented in NEC by surface patches of area 2x2 meters except for 15 patches at the location where the feed segment was connected. These 15 patches were created with an area of 2.4x1.3 meters to avoid inaccurate interactions between the feed wire and the connection surface. The feed segment which was connected between the horizontal upper notched surface and the perfectly conducting ground, was modeled with 3, 5, and 7 wire segments, which were fitted in the 4x2x12, 4x4x12 and 4x6x12 meter notches respectively. An E-gap voltage source was placed at the center of the feed wire. Figure 3.18 is a typical computer model representation of the 12x12x12 meter metal box, notched by a 4x4x12 meter volume.

Again, CPU time for the NEC calculations restricted the study and limited the number of the surface patches that could be used to model the three versions of the designed survivable antenna. The surface patch area in square wavelengths is presented in Table 2 of the previous section.

Average gain values close to two, for test frequencies from 2-10 MHz, are presented in Tables 5-7, corresponding to the three different notched sizes. The input impedance values resulting for each of these frequencies are also presented in these tables.

The average gain requirement was not satisfied for many of the frequencies, especially for the notched volumes of 4x4x12, and 4x6x12 meters. For the 4x2x12 meter notched volume model, values for 4.0-7.0 MHz were not presented, since the average gain values were unacceptable. The small notch, compared with the overall size of the metal box, seems satisfactory for the frequencies from 2.0 to 4.0 MHz, where the box size dominates. The bad average gain values for 4.0 to 7.0 MHz indicates errors or deficiencies in the numerical model. Since modeling guidelines are not violated, there is nothing at present that can properly explain the unacceptable average gain values.

For the 4x4x4 and 4x6x4 meter notched volume models, the range of frequencies with unacceptable average gain values was from 2.0 MHz up to about 6.0 MHz. Here the increased notched volume is still not yet electrically large enough, compared to wavelength for this range.

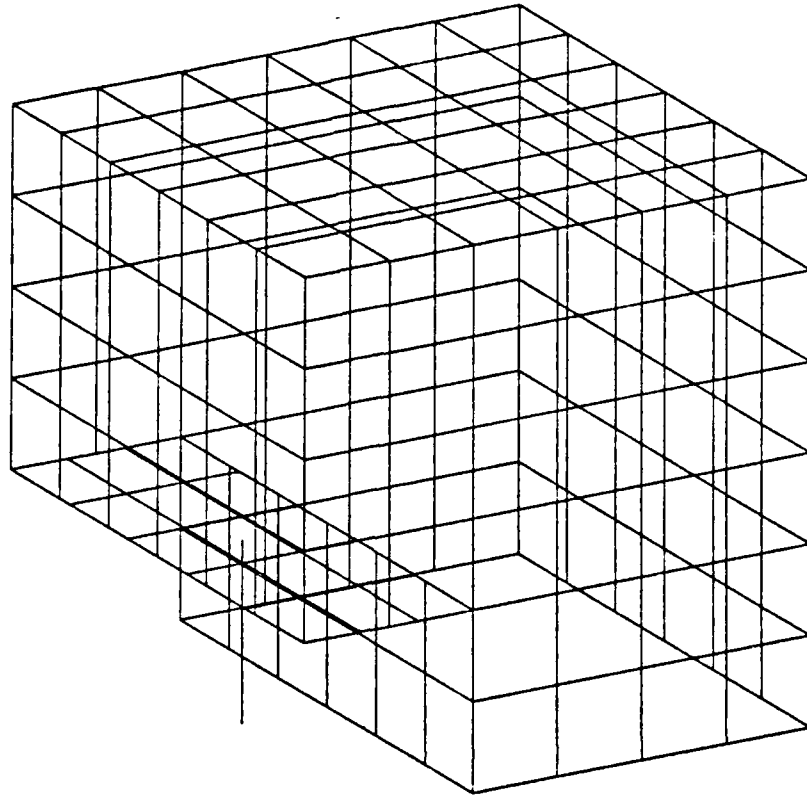


Figure 3.18 Computer Model of the 4x4x12 m Notched Volume Box

For all three survivable antenna versions, small notches produced low input impedance values. That is the reason that Smith chart plots for this antenna are not presented, since it was found that the 3:1 SWR criterion for practical operation, was satisfied only by frequencies very close to 10.0 MHz, for the 4x4x12 and 4x6x12 meter notched volume sizes. The 4x2x12 meter notched volume box was not matchable to the 3:1 SWR. The cause of this undesired property, was the continuously low resistance values of the input impedance, which did not exceed a normalized value of 0.75 in the Smith charts, even for a characteristic impedance of $50 + j0$ ohms.

For all three models presented in this section, elevation and azimuth radiation patterns were obtained for acceptable frequencies. For low frequencies

TABLE 5
 BOX NOTCHED BY A 4X2X12 METER VOLUME
 AVERAGE GAIN AND INPUT IMPEDANCE VALUES

Frequency (MHz)	Average Gain	Input Impedance (Ohms)
2.00	2.00	0.0729 + j124.5
2.44	1.94	0.118 + j111.0
2.99	1.92	0.175 + j102.0
3.65	2.17	0.152 + j97.21
8.17	2.16	2.704 + j124.8
10.00	1.94	8.64 + j147.9

TABLE 6
 BOX NOTCHED BY A 4X4X12 METER VOLUME
 AVERAGE GAIN AND INPUT IMPEDANCE VALUES

Frequency (MHz)	Average Gain	Input Impedance (Ohms)
6.68	2.12	4.26 + j175.0
8.17	1.96	10.6 + j214.4
10.00	1.91	22.5 + j268.1

the smaller notched volume of 4x2x12 meters, shows radiation patterns close to omnidirectional in shape. This property is desirable for an HF shipboard communications antenna. Figures 3.19 through 3.24 are typical plots for 2.0 - 4.0 MHz.

TABLE 7
 BOX NOTCHED BY A 4X6X12 METER VOLUME
 AVERAGE GAIN AND INPUT IMPEDANCE VALUES

Frequency (Mhz)	Average Gain	Input Impedance (Ohms)
6.68	2.01	9.30 + j259.8
8.17	1.92	19.2 + j329.0
10.00	1.91	37.0 + j432.2

As the frequency increases above 6.0 MHz, the radiation patterns are no longer as uniform in shape. From Figures 3.25 - 3.33, there is a null introduced at an elevation angle of about 30 degrees, on the side opposite the notch. The gain is also reduced for the secondary lobe. As the notched volume and the frequency are increased, the null occurs at the same elevation angle but it is now deeper with a slightly smaller secondary lobe. Horizontal patterns, for the null elevation angle have a cardioidal shape, with greatest gain in the direction of the notch, similar to the vertical patterns. The cardioidal shape and null become more pronounced as the frequency increases.

12X12X12 M BOX NOTCHED BY A 4X2X12 M VOLUME. FREQ = 2 MHZ

VERTICAL PATTERN (YZ PLANE), AZIMUTH ANGLE = 90 DEG.

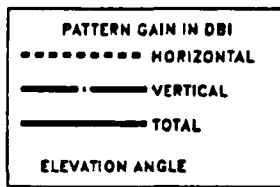
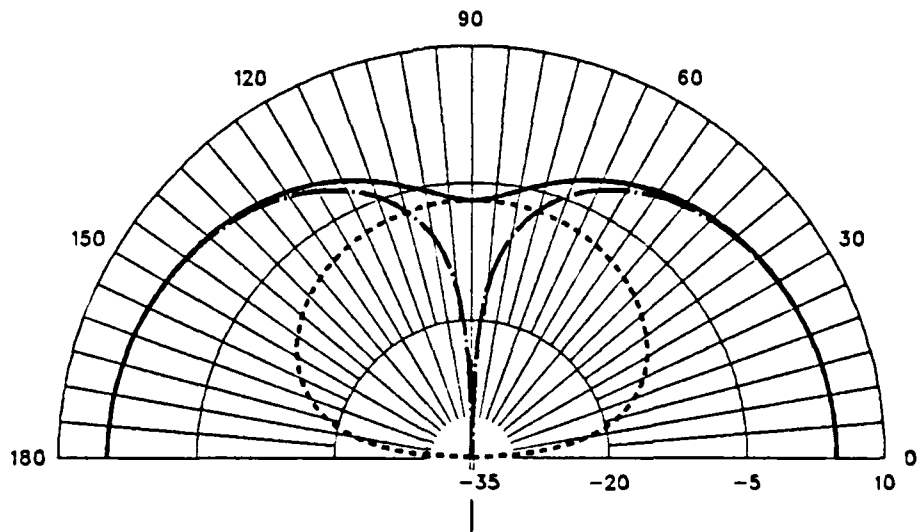


Figure 3.19 Vertical Pattern for Range 2.0-3.0 MHz. $\Phi = 90^\circ$

12X12X12 M BOX NOTCHED BY A 4X2X12 M VOLUME. FREQ = 2 MHZ

VERTICAL PATTERN (XZ PLANE), AZIMUTH ANGLE = 0 DEG.

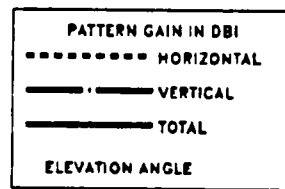
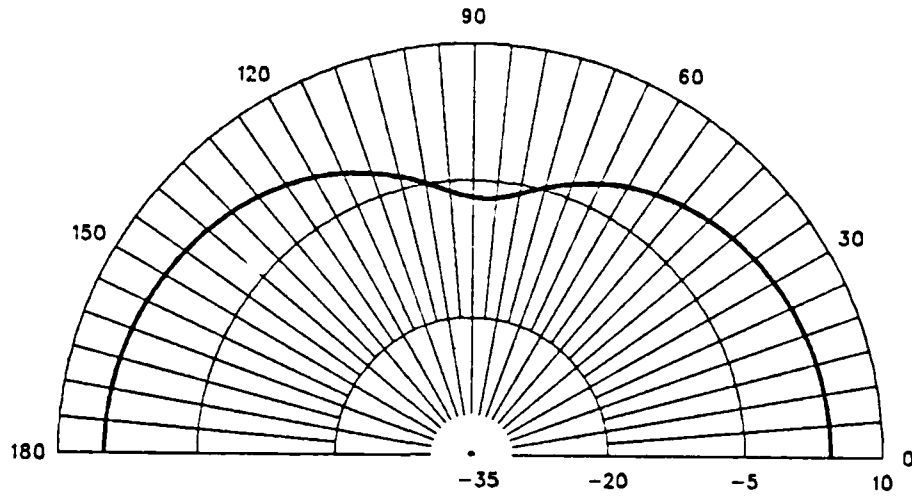


Figure 3.20 Vertical Pattern for Range 2.0-3.0 MHz. $\Phi = 0^\circ$

12X12X12 M BOX NOTCHED BY A 4X2X12 M VOLUME. FREQ = 2 MHZ

HORIZONTAL PATTERN (XY PLANE), ELEVATION ANGLE = 30 DEG.

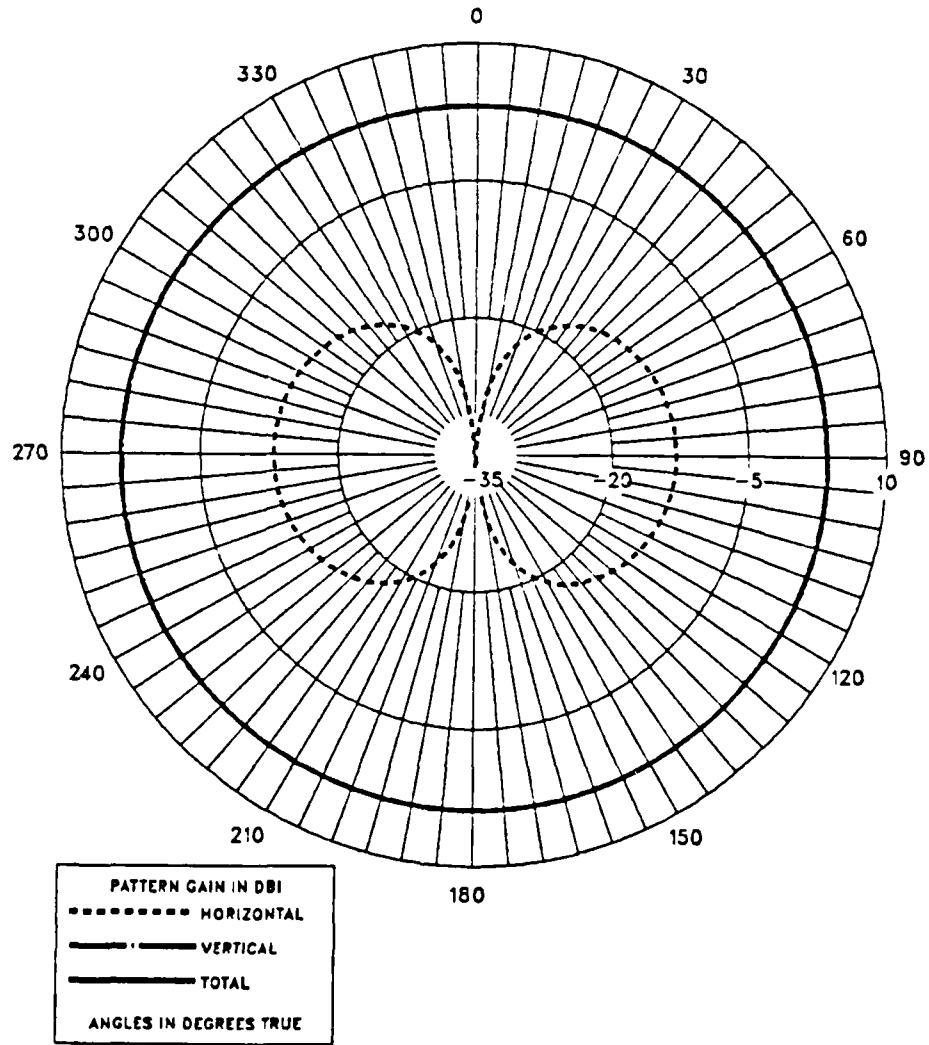


Figure 3.21 Elevation Pattern for Range 2.0-3.0 MHz

12X12X12 M BOX NOTCHED BY A 4X2X12 M VOLUME. FREQ = 3.6 MHZ

VERTICAL PATTERN (YZ PLANE), AZIMUTH ANGLE = 90 DEG.

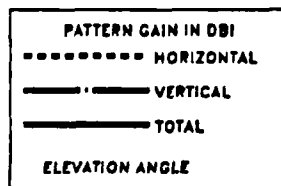
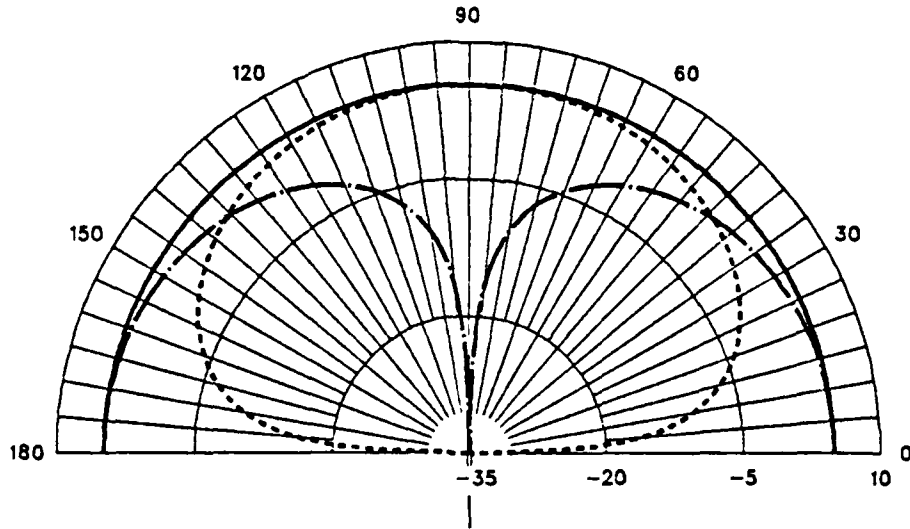


Figure 3.22 Vertical Pattern for Range 3.0-4.0 MHz. Phi = 90°

12X12X12 M BOX NOTCHED BY A 4X2X12 M VOLUME. FREQ = 3.6 MHZ

VERTICAL PATTERN (XZ PLANE), AZIMUTH ANGLE = 0 DEG.

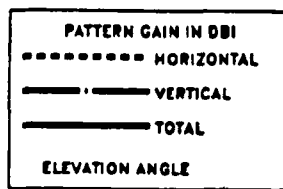
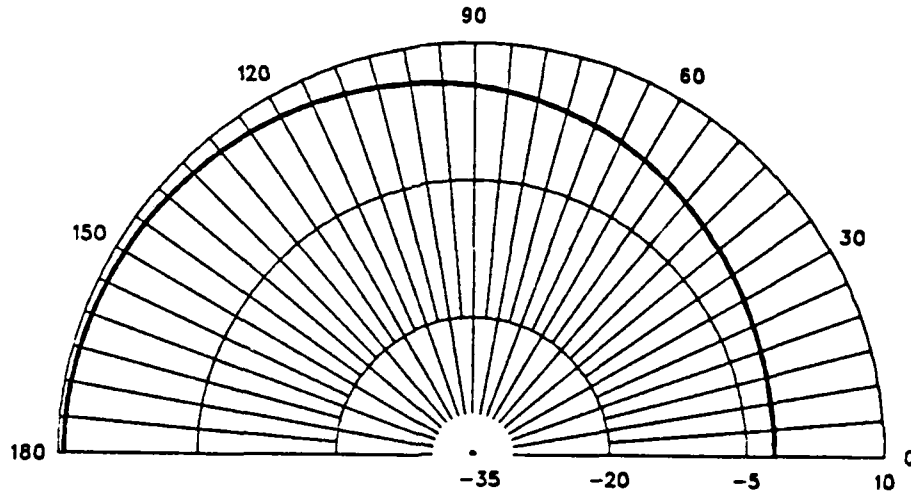


Figure 3.23 Vertical Pattern for Range 3.0-4.0 MHz. $\Phi = 0^\circ$

12X12X12 M BOX NOTCHED BY A 4X2X12 M VOLUME. FREQ = 3.6 MHZ

HORIZONTAL PATTERN (XY PLANE), ELEVATION ANGLE = 30 DEG.

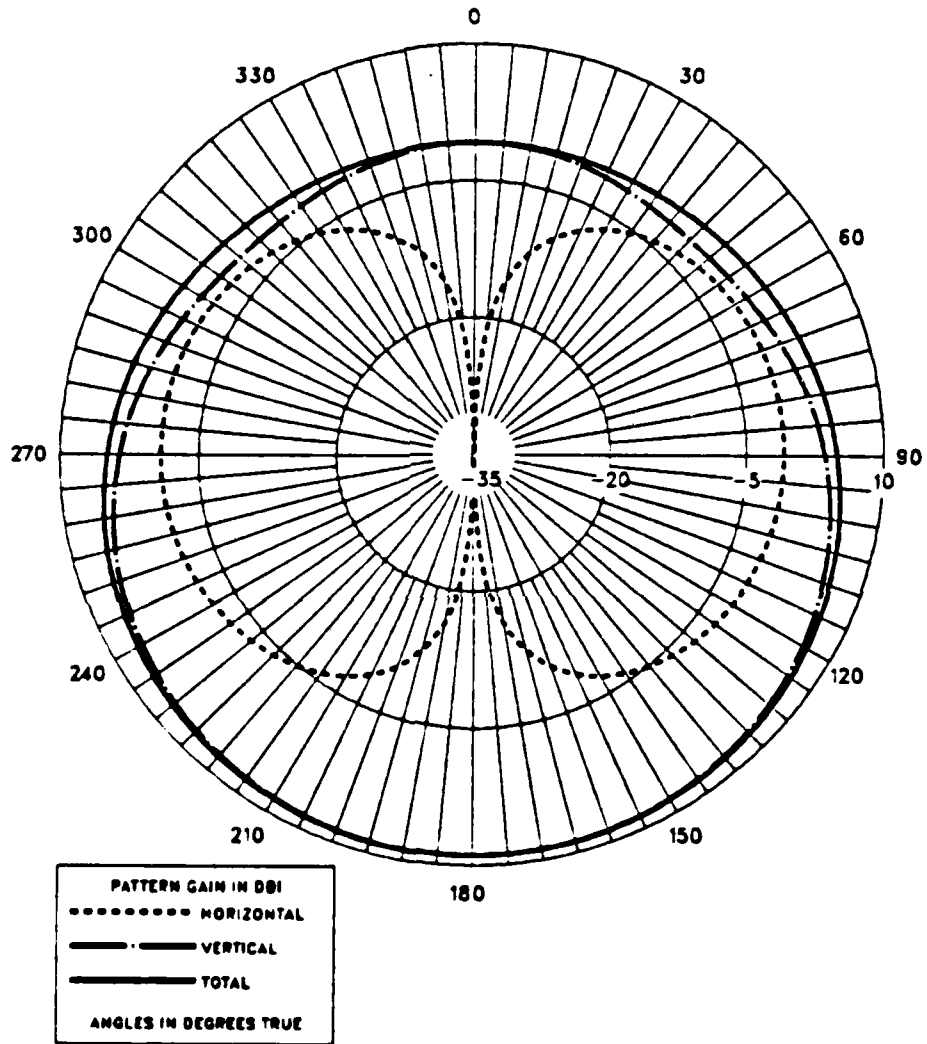


Figure 3.24 Elevation Pattern for Range 3.0-4.0 MHz

12X12X12 M BOX NOTCHED BY A 4X4X12 M VOLUME. FREQ = 6.6 MHZ

VERTICAL PATTERN (YZ PLANE), AZIMUTH ANGLE = 90 DEG.

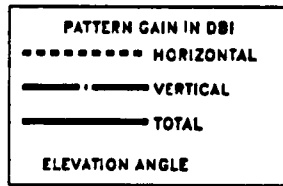
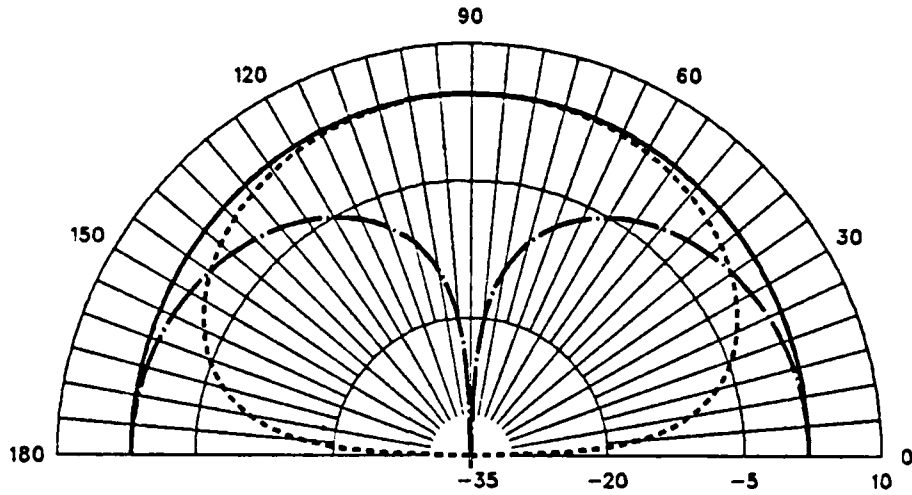


Figure 3.25 . Vertical Pattern for Range 6.0-7.5 MHz. Phi = 90°

12X12X12 M BOX NOTCHED BY A 4X4X12 M VOLUME. FREQ = 6.6 MHZ

HORIZONTAL PATTERN (XY PLANE), ELEVATION ANGLE = 30 DEG.

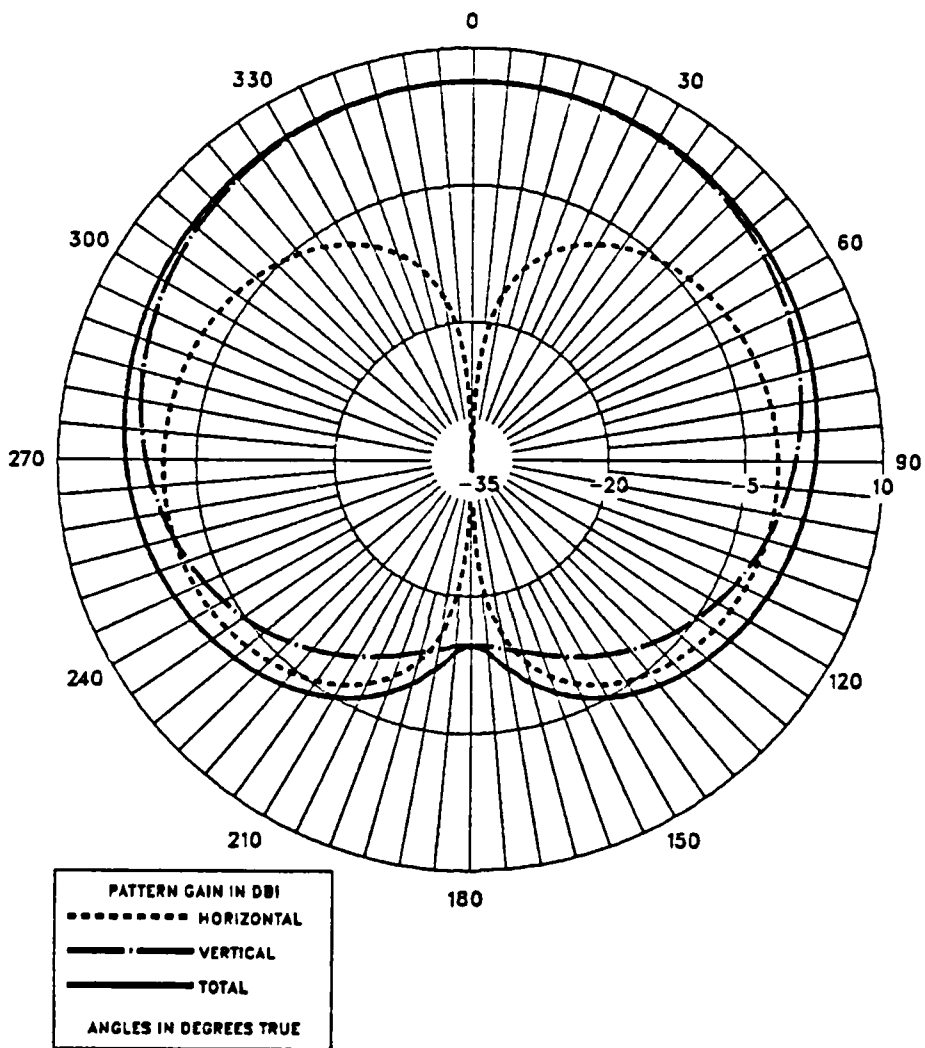


Figure 3.26 Vertical Pattern for Range 6.0-7.5 MHz. $\Phi = 0^\circ$

12X12X12 M BOX NOTCHED BY A 4X4X12 M VOLUME. FREQ = 6.6 MHZ

VERTICAL PATTERN (XZ PLANE), AZIMUTH ANGLE = 0 DEG.

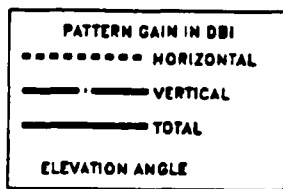
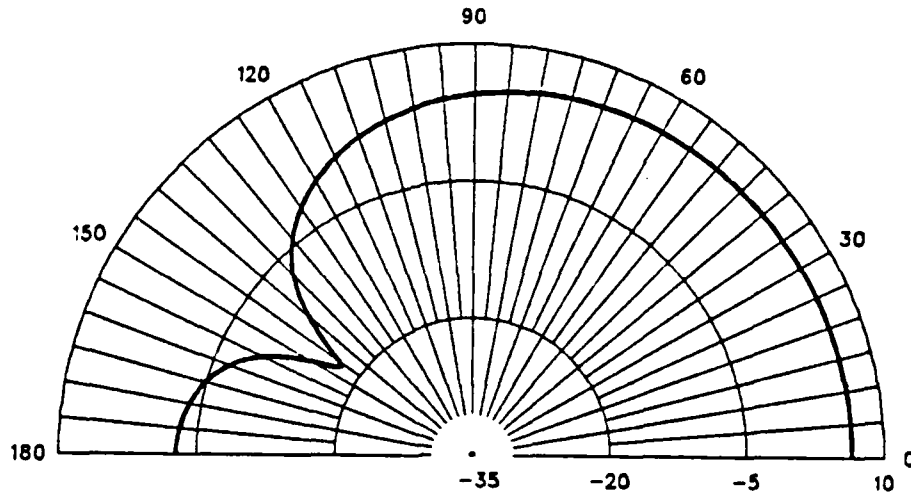


Figure 3.27 Elevation Pattern for Range 6.0-7.5 MHz

12X12X12 M BOX NOTCHED BY A 4X2X12 M VOLUME. FREQ = 8.1 MHZ

VERTICAL PATTERN (YZ PLANE), AZIMUTH ANGLE = 90 DEG.

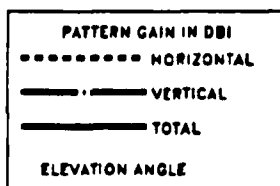
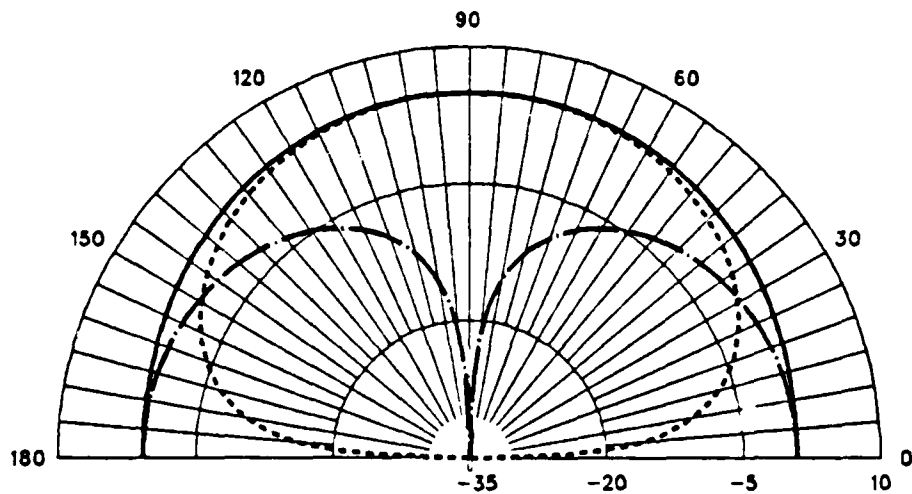


Figure 3.28 Vertical Pattern for Range 7.5-9.0 MHz. $\Phi = 90^\circ$

12X12X12 M BOX NOTCHED BY A 4X2X12 M VOLUME. FREQ = 8.1 MHZ

VERTICAL PATTERN (XZ PLANE), AZIMUTH ANGLE = 0 DEG.

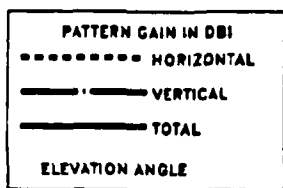
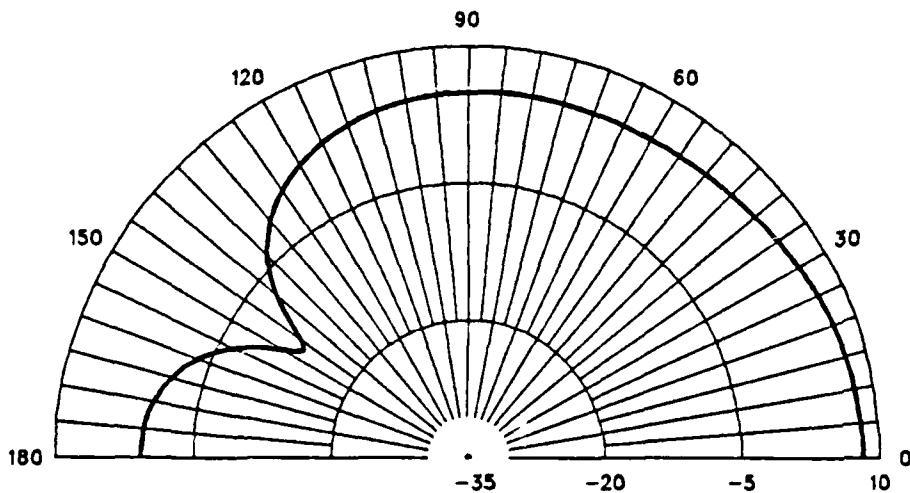


Figure 3.29 Vertical Pattern for Range 7.5-9.0 MHz. $\Phi = 0^\circ$

12X12X12 M BOX NOTCHED BY A 4X2X12 M VOLUME. FREQ = 8.1 MHZ

HORIZONTAL PATTERN (XY PLANE), ELEVATION ANGLE = 30 DEG.

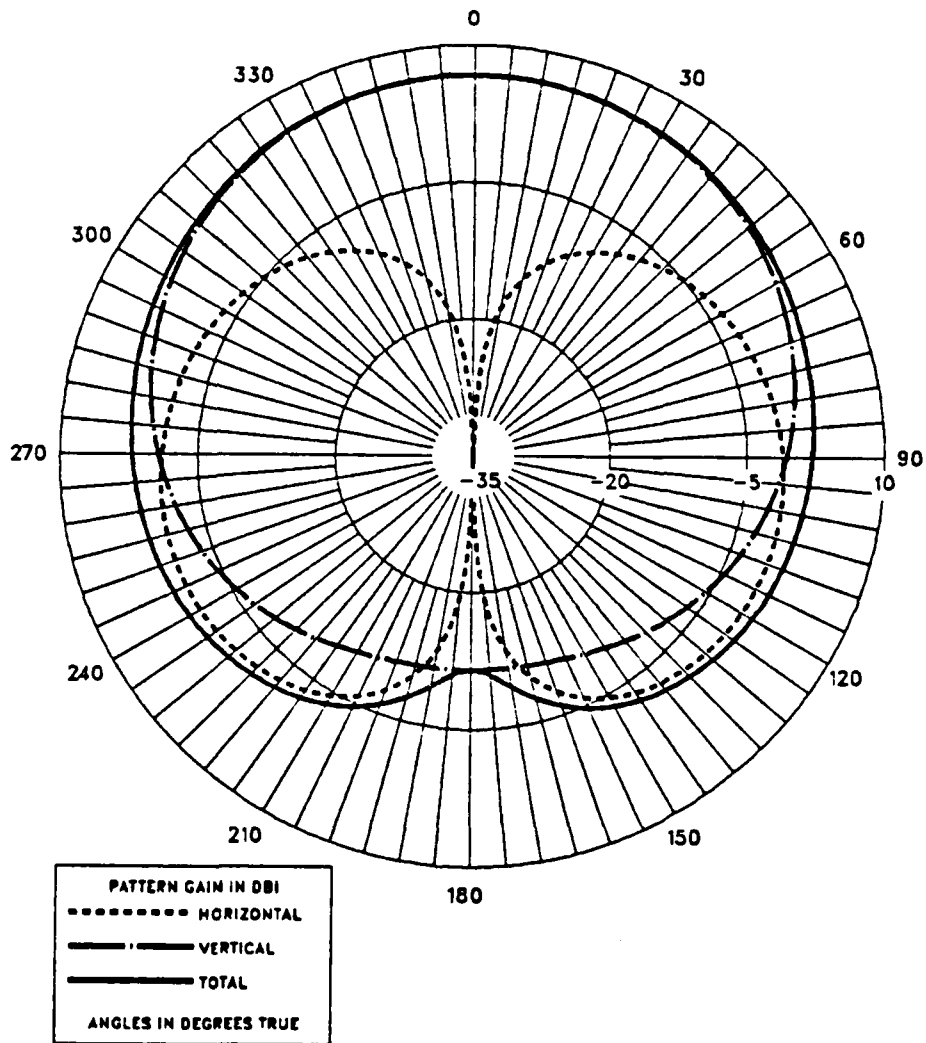


Figure 3.30 Elevation Pattern for Range 7.5-9.0 MHz

12X12X12 M BOX NOTCHED BY A 4X6X12 M VOLUME. FREQ = 10 MHZ

VERTICAL PATTERN (YZ PLANE), AZIMUTH ANGLE = 90 DEG.

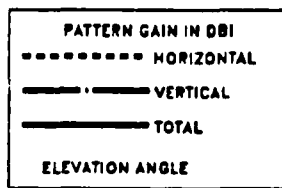
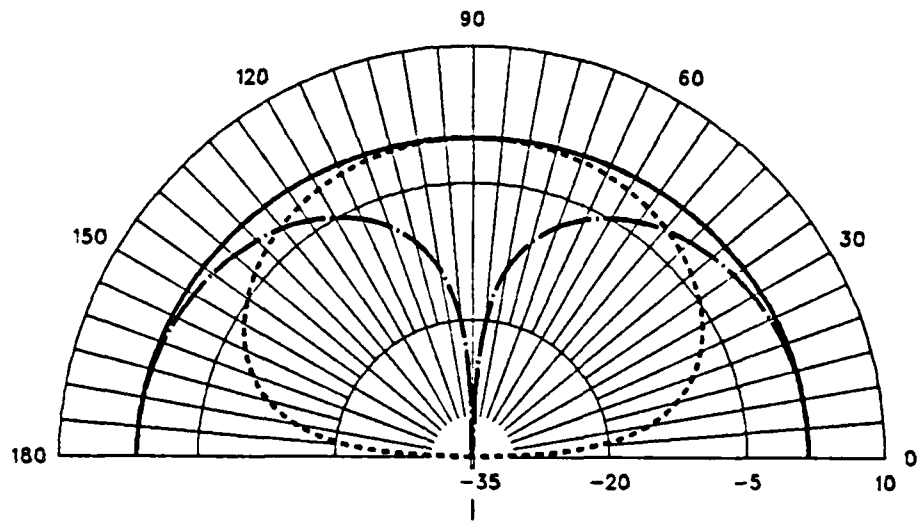


Figure 3.31 Vertical Pattern for Range 9.0-10.0 MHz. $\Phi = 90^\circ$

12X12X12 M BOX NOTCHED BY A 4X6X12 M VOLUME. FREQ = 10 MHZ

VERTICAL PATTERN (XZ PLANE), AZIMUTH ANGLE = 0 DEG.

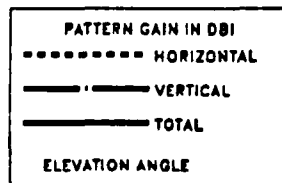
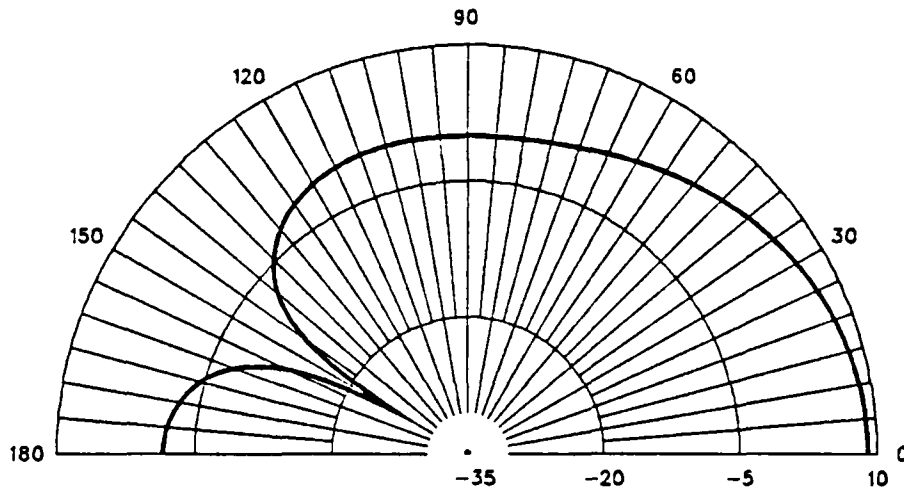


Figure 3.32 Vertical Pattern for Range 9.0-10.0 MHz. $\Phi = 0^\circ$

12X12X12 M BOX NOTCHED BY A 4X6X12 M VOLUME. FREQ = 10 MHZ

HORIZONTAL PATTERN (XY PLANE), ELEVATION ANGLE = 30 DEG.

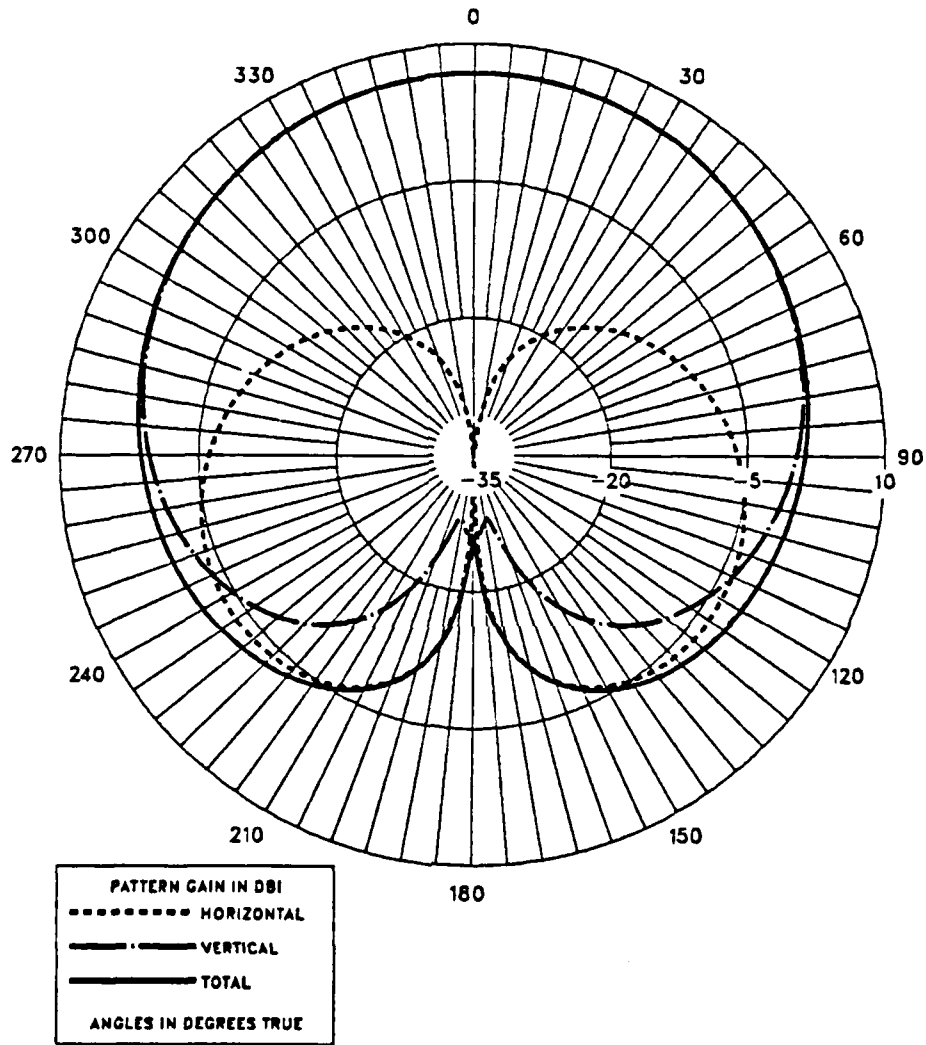


Figure 3.33 Elevation Pattern for Range 9.0-10.0 MHz

IV. CONCLUSIONS AND RECOMMENDATIONS

This study has proposed two survivable HF communication antenna designs and developed computer models for them which were used to determine the input impedance and radiation patterns of the antennas over the HF range of 2-10 MHz. Both antennas used surface patches to represent their metallic closed surfaces. A wire grid was used to model the surface of the patch monopole which was placed near a metal box, for one design. In the other design, notched volumes of various sizes, were placed in one end of the base of a metal box, and excited via a short wire segment.

A. CONCLUSIONS

Computed input impedance, using NEC, is affected mainly by the geometry representation of each model (which can be validated by average gain results), the type of voltage source, the number of feed segments, the radius of the wires, and the area of the subdivided patches if the feed wire is connected to a surface patch.

For a wire grid, as used in modeling the patch monopole, a grid spacing of 0.1 wavelengths is usually adequate. Since models with tighter grid densities yield impedances closer to measured values, the grid density that was selected, was less than 0.03 wavelengths at all frequencies.

For a surface patch, an area of 0.04 square wavelengths is usually adequate for representing a closed surface with non-vanishing volume, like the metal box that was modeled in both configurations. Again the accuracy of the input impedance improves as patch density is increased. For both configurations the surface patch area did not exceed the value of 0.004 square wavelengths.

For this study, the object sizes in wavelengths were small enough to require the use of 64-bit word-size for the computer used with NEC. This forced the use of double precision on the NPS IBM 3033 system, which increased computation time requirements substantially.

NEC can model antenna surfaces successfully, and can produce computed results close to physical measurements. Since there are many factors affecting

the accuracy of the computer models results, it is often necessary to build physical models and to measure the performance parameters of the antenna as an aid in establishing valid numerical models.

The results of this thesis indicate that a rectangular volume driven by a patch monopole, placed at various spacings from any of the volumes faces, does possess radiation patterns and impedance characteristics which make it a feasible design for a small but useful part of the design range of frequencies. This antenna is matchable to a 3:1 SWR over the frequency range of about 8 MHz to 10 MHz, with the use of series reactances. For small electrical heights, less than 0.1 wavelengths, the radiation patterns are similar to those of a 0.25 wavelength monopole. This was an expected result, since antennas with small electrical heights produce similar radiation patterns. The patterns become more uniform for electrical heights greater than about 0.2 wavelengths, and also are compressed in the plane of the antenna. For electrical heights above 0.4 wavelengths, the patterns are more directional towards the patch monopole side. The box had a dominant effect for all radiation patterns since they were almost identical for the same frequency when the spacing of the patch monopole from the box was varied.

The notched box configuration results indicate that a notched rectangular volume possesses radiation patterns and input impedance characteristics which make it useable only for a small part of the test frequency range. This antenna, for notched volume sizes of 4x4x12 meters and 4x6x12 meters, is matchable to a 3:1 SWR for frequencies very close to 10 MHz, and possibly higher, with the use of series reactances. The radiation patterns, though very similar to each other, indicate that there is almost uniform radiation for low frequencies (or small electrical heights) and increased directionality towards the notch side of the antenna for higher frequencies, but with an exchange of null towards the side opposite the notch. The similarity of radiation patterns for different notched volumes, at the same frequencies, indicates that the box size dominates over any of the three different notched sizes.

B. RECOMMENDATIONS

For both survivable antenna configurations, there are some aspects needing further study :

- The antennas' impedance values and radiation patterns should be investigated for a higher frequency range to determine if improvement in performance which are observed approaching 10 MHz, continue beyond 10 MHz.
- The patch monopole size and the notch volume should be increased until they override the dominant effect of the box.
- The effect of less dense wire grid and larger surface patches on a computed antenna model result, should be investigated for possible saving of computer storage and computing time requirements.
- Standard methods of feed point impedance multiplication or increase (i.e. folding, etc.) for the feed wires, and the location of the feed segment attachment point in the notched volume, should be investigated.
- Overly-directional patterns obtained at higher frequencies might be smoothed by multiple-patch or multiple notched volumes.
- A separate investigation is needed for establishing reasons for poor average gain for the "mid-frequencies" in the notched volume antenna.
- Finally, physical models of both survivable antennas, should be built, for comparison with the computer model results.

APPENDIX

INPUT DATA SETS USED FOR THE MODELED ANTENNAS

1. The following job card listing is typical for computing average gain for the patch monopole in front of the metal box.

```
BX1HAV JOB (0722.0305), NEC RUN, CLASS = J
*MAIN LINES = (9999)
NEC      PROC VERSION = DNP2000, STORAGE = 3096K
GO       EXEC PGM = &VERSION, REGION = &STORAGE
STEPLIB DD DISP = SHR, DSN = MSS.FI595, NEC, LOAD
         DD DISP = SHR, DSN = SYS1.VFORTLIB
FT01F001 DD DUMMY
FT04F001 DD UNIT = SYSDA, SPACE = (CYL,(8,2)),
         DCB = (RECFM = VBS, BLKSIZE = 19069)
FT05F001 DD DDNAME = SYSIN
FT06F001 DD SYSOUT = *
FT08F001 DD DUMMY
FT11F001 DD UNIT = SYSDA, SPACE = (CYL,(8,2)),
         DCB = (RECFM = VBS, BLKSIZE = 19069)
FT12F001 DD UNIT = SYSDA, SPACE = (CYL,(8,2)),
         DCB = (RECFM = VBS, BLKSIZE = 19069)
FT13F001 DD UNIT = SYSDA, SPACE = (CYL,(8,2)),
         DCB = (RECFM = VBS, BLKSIZE = 19069)
FT14F001 DD UNIT = SYSDA, SPACE = (CYL,(8,2)),
         DCB = (RECFM = VBS, BLKSIZE = 19069)
FT15F001 DD UNIT = SYSDA, SPACE = (CYL,(8,2)),
         DCB = (RECFM = VBS, BLKSIZE = 19069)
FT16F001 DD UNIT = SYSDA, SPACE = (CYL,(8,2)),
         DCB = (RECFM = VBS, BLKSIZE = 19069)
FT20F001 DD UNIT = SYSDA, SPACE = (CYL,(8,2)),
         DCB = (RECFM = VBS, BLKSIZE = 19069)
FT21F001 DD DUMMY
        PEND
```

STEPNAME EXEC NEC.VERSION = DNPG2000,STORAGE = 3096K
GO.FT08F001 DD DSN = MSS.S0722.PATCH.PLOTDATA(BX1HAV),
DISP = (OLD.KEEP).
DCB = (RECFM = FB,LRECL = 80,BLKSIZE = 12960,DSORG = PO,
GO.SYSIN DD *

CM THIS IS A 12X12X12 MTS BOX OVER PERFECT GROUND.
CM MADE WITH PATCHES 2X2 M EACH.AT DISTANCE 1.5 M
CE FROM A PATCH 10x10 M. FREQ = 2-10 MHZ

GW 200.10.7.5.-5.1.7.5.5.1..05

GM 0.10.0.0.0.0.0.1.200

GW 300.10.7.5.-5.1.7.5.-5.11..05

GM 0.10.0.0.0.0.1.0.300

GW 400.1.7.5.0.0.7.5.0.1..05

SM 6.6.6.6.0.-6.6.0 RIGHT SIDE

SC 0.0.-6.6.12

SM 6.6.6.6.12.-6.6.12 UP FACE

SC 0.0.-6.-6.12

SM 6.6.6.-6.0.6.6.0 FRONT FACE

SC 0.0.6.6.12

SM 6.6.-6.6.0.-6.-6.0 BACK FACE

SC 0.0.-6.-6.12

SM 6.6.-6.-6.0.6.-6.0 LEFT SIDE

SC 0.0.6.-6.12

GP

GE 1

GN 1

EX 0.400.1.00.1

FR 1.9.0.0.2.1.2228445

PT -1.1.1.1

RP 0.10.4.1512.0.0.10.60

XQ

EN

.

.

2. The following job card listing is typical for computing radiation patterns for the patch monopole in front of the box.

```
BXPCH1H2 JOB (0722,0305), 'NEC RUN', CLASS = G
*MAIN LINES = (9999)
NEC      PROC VERSION = DNPG2000, STORAGE = 3096K
GO      EXEC PGM = &VERSION, REGION = &STORAGE
STEPLIB DD DISP = SHR, DSN = MSS.F1595.NEC.LOAD
        DD DISP = SHR, DSN = SYS1.VFORTLIB
FT01F001 DD DUMMY
FT04F001 DD UNIT = SYSDA, SPACE = (CYL,(8,2)),
        DCB = (RECFM = VBS, BLKSIZE = 19069)
FT05F001 DD DDNAME = SYSIN
FT06F001 DD SYSOUT = *
FT08F001 DD DUMMY
FT11F001 DD UNIT = SYSDA, SPACE = (CYL,(8,2)),
        DCB = (RECFM = VBS, BLKSIZE = 19069)
FT12F001 DD UNIT = SYSDA, SPACE = (CYL,(8,2)),
        DCB = (RECFM = VBS, BLKSIZE = 19069)
FT13F001 DD UNIT = SYSDA, SPACE = (CYL,(8,2)),
        DCB = (RECFM = VBS, BLKSIZE = 19069)
FT14F001 DD UNIT = SYSDA, SPACE = (CYL,(8,2)),
        DCB = (RECFM = VBS, BLKSIZE = 19069)
FT15F001 DD UNIT = SYSDA, SPACE = (CYL,(8,2)),
        DCB = (RECFM = VBS, BLKSIZE = 19069)
FT16F001 DD UNIT = SYSDA, SPACE = (CYL,(8,2)),
        DCB = (RECFM = VBS, BLKSIZE = 19069)
FT20F001 DD UNIT = SYSDA, SPACE = (CYL,(8,2)),
        DCB = (RECFM = VBS, BLKSIZE = 19069)
FT21F001 DD DUMMY
        PEND
STEPNAME EXEC NEC, VERSION = DNPG2000, STORAGE = 3096K
GO.FT08F001 DD DSN = MSS.S0722.PATCH.PLOTDATA(BXPCH1H2).
```

```

DISP=(OLD,KEEP),
DCB=(RECFM=FB,LRECL=80,BLKSIZE=12960,DSORG=PO)
GO.SYSIN DD *
CM THIS IS A 12X12X12 M BOX OVER PERFECT GROUND,
CM MADE WITH PATCHES 2X2 M EACH,AT DISTANCE 1.5 M
CM FROM A PATCH 10x10 M. FREQ = 2 MHZ.
CE NGF DATA WILL BE USED FOR PLOTTINGS DATA.
GW 200,5,7.5,0,1,7.5,5,1,.05
GM 0,10,0,0,0,0,0,1,200
GW 300,10,7.5,1,1,7.5,1,11,.05
GM 0,4,0,0,0,0,1,0,300
SM 6,6,6,6,0,-6,6,0          RIGHT SIDE
SC 0,0,-6,6,12
SM 6,3,6,6,12,-6,6,12      UP HALF FACE
SC 0,0,-6,0,12
SM 3,6,6,0,0,6,6,0        FRONT HALF FACE
SC 0,0,6,6,12
SM 3,6,-6,6,0,-6,0,0      BACK HALF FACE
SC 0,0,-6,0,12
GX 0,010
GP
GE 1
GN 1
FR 0,0,0,0,2
WG
NX
CM THE PATCH MONOPOLE'S CENTER GRID LINE AND THE
CM FEED LINE ARE NOW CONNECTED
GF
GW 400,10,7.5,0,1,7.5,0,11,.05
GW 500,1,7.5,0,0,7.5,0,1,.05
GP
GE 1
EX 0,500,1,00,1
PL 3,1,0,4

```

PT -1,1,1,1
RP 0,181,1,1010,-90,90,1,0
PL 3,1,0,4
PT -1,1,1,1
RP 0,181,1,1010,-90,0,1,0
PL 3,2,0,4
PT -1,1,1,1
RP 0,1,361,1010,60,0,0,1
XQ
EN
*
*

3. The following job card listing is typical for computing average gain of a 12x12x12 meter box, notched by a 4x4x12 meter volume. The same data cards except for additional radiation pattern (RP) cards, and plotting (PL) cards, were used for radiation patterns.

```
BXCTAV2    JOB (0722,0305), 'NEC RUN', CLASS = G
NEC        PROC VERSION = DNP2000, STORAGE = 3096K
GO         EXEC PGM = &VERSION, REGION = &STORAGE
STEPLIB   DD DISP = SHR, DSN = MSS.F1595.NEC.LOAD
          DD DISP = SHR, DSN = SYS1.VFORTLIB
FT01F001  DD DUMMY
FT04F001  DD UNIT = SYSDA, SPACE = (CYL,(8,2)),
          DCB = (RECFM = VBS, BLKSIZE = 19069)
FT05F001  DD DDNAME = SYSIN
FT06F001  DD SYSOUT = *
FT08F001  DD DUMMY
FT11F001  DD UNIT = SYSDA, SPACE = (CYL,(8,2)),
          DCB = (RECFM = VBS, BLKSIZE = 19069)
FT12F001  DD UNIT = SYSDA, SPACE = (CYL,(8,2)),
          DCB = (RECFM = VBS, BLKSIZE = 19069)
FT13F001  DD UNIT = SYSDA, SPACE = (CYL,(8,2)).
```

```

      DCB=(RECFM=VBS,BLKSIZE=19069)
FT14F001 DD UNIT=SYSDA,SPACE=(CYL,(8,2)),
      DCB=(RECFM=VBS,BLKSIZE=19069)
FT15F001 DD UNIT=SYSDA,SPACE=(CYL,(8,2)),
      DCB=(RECFM=VBS,BLKSIZE=19069)
FT16F001 DD UNIT=SYSDA,SPACE=(CYL,(8,2)),
      DCB=(RECFM=VBS,BLKSIZE=19069)
FT20F001 DD UNIT=SYSDA,SPACE=(CYL,(8,2)),
      DCB=(RECFM=VBS,BLKSIZE=19069)
FT21F001 DD DUMMY
      PEND
STEPNAME EXEC NEC.VERSION=DNPG2000.STORAGE=3096K
GO FT08F001 DD DSN=MSS.S0722.BXCUT.PLOTDATA(BXCTAV2),
      DISP=(OLD,KEEP),
      DCB=(RECFM=FB,LRECL=80,BLKSIZE=12960,DSORG=PO)
GO SYSIN DD *

```

CM THIS IS A 12X12X12 M BOX WITH A NOTCH 4X2X12 M OVER
CM PERFECT GROUND PLANE.SURFACES ARE REPRESENTED BY
CM PATCHES EACH HAVING AN AREA 2X2 SQ M. EXCEPT OF 15
CM LOCATED AT THE UPPER BOTTOM FACE THAT THE FEED LINE
CM IS THE AREA OF THESE 15 PATCHES IS 2.4X1.33 SQ M.

CE FREQ = 5.46-8.17 MHZ.

SM 6,6,-6,6,0,-6,-6,0	BACK FACE
SC 0,0,-6,-6,12	
SM 6,6,6,-6,12,6,6,12	UPPER FACE
SC 0,0,-6,6,12	
SM 4,6,2,6,0,-6,6,0	RIGHT 2-3 SIDE
SC 0,0,-6,6,12	
SM 4,6,-6,-6,0,2,-6,0	LEFT 2-3 SIDE
SC 0,0,2,-6,12	
SM 2,5,6,6,2,2,6,2	RIGHT 5-18 SIDE
SC 0,0,2,6,12	
SM 2,5,2,-6,2,6,-6,2	LEFT 5-18 SIDE
SC 0,0,6,-6,12	
SM 6,5,6,-6,2,6,6,2	FRONT UP 5-6 SIDE

SC 0,0,6,6,12

SM 6.1.2,-6.0.2,6.0

SC 0.0.2.6.2

SM 5.3.6,6.2,6.-6.2

SC 0.0.2,-6.2

GW 10.3,4.0.0.4.0.2..05

GP

GE 1

GN 1

EX 0.10.2.00.1

FR 1.3.0.0.5.468,1.2228

PT -1.1.1.1

RP 0.19.13.1512.0.0.5.15

XQ

EN

.

.

FRONT UP 1.6 SIDE

UPPER BOTTOM 1.3 FACE

FEED LINE

LIST OF REFERENCES

1. Tertocha, James C., *A Feasibility Study of a Shipboard Combat Survivable HF Antenna Design*, Naval Postgraduate School, Monterey, CA, March 1986.
2. Naval Ocean Systems Center Technical Document 116, *Numerical Electromagnetics Code (NEC) - Method of Moments*, by G.J. Bruke and A.J. Poggio, January 1981.
3. Bruke, J.G., Poggio, A.J., Logan, J.C., and Rockway, J.W., *Numerical Electromagnetics Code - A Program For Antenna System Analysis*, EMC Symposium and Exhibition, Rotterdam, The Netherlands, May 1-3, 1979.
4. Harrington, Roger F., *Field Computation By Moment Methods*, MacMillan Company, New York, 1968.
5. Balanis, Constantine A., *Antenna Theory Analysis and Design*, Harper and Row Inc., 1982.

BIBLIOGRAPHY

Brown, R.G., Sharpe, R.A., Huges, W.L., Post, R.E., *Lines, Waves, and Antennas*, John Wiley and Sons, Inc., 1961,1973.

Cheng, David K., *Field and Wave Electromagnetics*, Addison-Wesley Publishing Company, 1984.

Jasik, H., *Antenna Engineering Handbook*, McGraw-Hill Book Company, 1961.

Stutzman, Warren L., Theile, Gary A., *Antenna Theory and Design*, John Wiley And Sons, Inc., 1983.

INITIAL DISTRIBUTION LIST

		No. Copies
1.	Defence Technical Information Center Cameron Station Alexandria, VA 22304-6145	2
2.	Library, Code 0142 Naval Postgraduate School Monterey, CA 93943-5002	2
3.	Department Chairman, Code 62 Department of Electrical and computer Engineering Naval Postgraduate School Monterey, CA 93943-5000	1
4.	Dr. Richard W. Adler, Code 62Ab Department of Electrical and Computer Engineering Naval Postgraduate School Monterey, CA 93943-5000	5
5.	Dr. Harry Atwater, Code 62An Department of Electrical and Computer Engineering Naval Postgraduate School Monterey, CA 93943-5000	1
6.	Hellenic Navy General Staff 2nd Branch, Education Department Stratopedon Papagou GR 155.61 - Holargos, GREECE	4
7.	LT Ioannis G. Vorrias, H.N. Larnakos 36 GR 156.69 - Papagos, GREECE	5
8.	Al Christman / Roger Radcliff Ohio University, Clippinger Res. Labs Athens, OH 45701	1
9.	Harold Askins NESEC - Charleston 4600 Goer Rd. N. Charleston, SC 29406	1
10.	W.P. Averill, CAPT. U.S. NAVAL ACADEMY, Department of Electrical Engineering Annapolis, MD 21402	1
11.	J.K. Breakall Lawrence Liv. Nat'l. Lab. P.O. Box 5504, L-156 Livermore, CA 94550	1
12.	Mr. Jim Logan, NOSC Code 822(T) 271 Catalina Blvd. San Diego, CA 92152	1
13.	I.C. Olson, NOSC Code 822(T) 271 Catalina Blvd. San Diego, CA 92152	1

14. R. Raschke, GE Elec Co, BLDG 3, RM 3312
P.O. Box 2500
Daytona Beach, FL 32015 1
15. J.J. Reaves JR., Naval Elec. Sys. Eng. Cntr.
4600 Marriott Dr.
N. Charleston, SC 29413 1
16. Alfred Resnick, Capital Cities Comm./ABC Radio
1345 Ave. of Americas 26th Floor
New York, NY 10105 1
17. John W. Rockway, NOSC Code 822(T)
271 Catalina Blvd.
San Diego, CA 92152 1
18. E. Thowless, NOSC Code 822(T)
271 Catalina Blvd.
San Diego, CA 92152 1
19. W.F. Flanigan, NOSC Code 825
271 Catalina Blvd.
San Diego, CA 92152 1
20. M. Selkellick, Code 825
David Taylor Naval Ship Research
Development Center
Bethesda, MD 20084-5000 1
21. D. Washburn, Code 822
Naval Ocean Systems Center
271 Catalina Blvd.
San Diego, CA 92152 1
22. Robert Latorre
Lawrence Liv. Nat'l. Lab.
P.O. Box 5504, L-156
Livermore, CA 94550 1
23. Ron Corry
USAISEA ASBH-SET-P
Fort Huachuca, AR 85613-5300 1
24. Bill Alvarez
USAISEA ASBH-SET-P
Fort Huachuca, AR 85613-5300 1
25. Janet McDonald
USAISEA ASBH-SET-P
Fort Huachuca, AR 85613-5300 1
26. Dr. Tom Tice
Department of Electrical and Computer Engrg.
Arizona State University
Tempe, AR 85287 1
27. Dr. Roger C. Rudduck
Ohio State University
Electrophysics Laboratory
1320 Kinnear Rd.
Colombus, OH 43212 1
28. Commander Naval Space and
Naval Warfare Systems Command
Attention: Dick Pride
PDW 110-243
Washington D.C. 20363 1

29. Naval Sea Systems Command
Attention: P. Law
C61X41
Washington D.C. 20362 1
30. James Tertocha
C-15 Tenbytowne Apts.
Delran, NJ 08075 1
31. LT Dimitris Koutsouras, H.N.
250 Forest Ridge, #72
Monterey, CA 93940 1
32. LT George Lymberopoulos, H.N.
Ferron St. 48-50
Athens 104.40, GREECE 1
33. LCDR Mario Cabral Neiva
Brazilian Naval Commision
4706 Wisconsin Ave., N.W.
Washington D.C. 20016 1
34. LT Hussain Safraz, P.N.
1577 18 F.B. AREA
Karachi, PAKISTAN 1
35. Director Research Administration, Code 012
Naval Postgraduate School
Monterey, CA 93943-5000 1

END

5-87

DTIC